Life-cycle cost-based risk assessment of aging bridge networks

Matteo Maria Messore, Luca Capacci*, Fabio Biondini

Department of Civil and Environmental Engineering, Politecnico di Milano

Piazza Leonardo da Vinci 32, 20133 Milan, Italy

* Corresponding author: luca.capacci@polimi.it

Life-cycle cost-based risk assessment of aging bridge networks

Abstract

Road infrastructures and bridge networks are becoming increasingly complex systems due to the development of technology in transportation engineering and the continual growth of urban communities. Infrastructure disservice due to seismic events may lead to unacceptable discomfort for commuters. Moreover, network downtime results into economic losses for the affected community, to be quantified in monetary terms by user costs. Seismically vulnerable bridges are also affected by environmental agents that can reduce their structural performance over time. This paper presents a comprehensive life-cycle cost-based probabilistic framework for seismic risk assessment of spatially distributed aging bridge networks. The seismic risk measure is formulated in terms of annual exceedance rate of a target threshold of user costs. The methodology is applied to a road system in Lombardy region, Italy, reproducing network connectivity and daily travel demands among four major cities and smaller neighbouring municipalities. Despite the fact that the area of interest is characterized by low seismicity, the results allow to quantify the impact of environmental deterioration in exacerbating the network seismic risk, highlighting the need for a life-cycle-informed approach to optimal management of infrastructure systems.

Keywords: seismic risk, life-cycle assessment, road networks, aging bridges, user cost

Introduction

In consequence of technology development processes in transportation engineering and continual growth of urban communities, road infrastructure systems and bridge networks are becoming increasingly complex. Transportation systems are essential lifelines for the operability of small to large businesses, as well as for the mobility of daily commuters and travelers. Therefore, connectivity of transportation networks plays a key role in social communities' daily life and sustainable growth (Sierra et al. 2018). In road networks, bridges usually represent the most vulnerable components to seismic action (Hwang et al. 2000, Banerjee and Shinozuka 2008, Carturan et al. 2013), built to overcome physical or manmade obstacles with lack of fast detouring when they undergo operational disruption. Their construction, adequate maintenance and prompt repair in the aftermath of eventual damage have considerable social impacts (Navarro et al. 2018). Out-of-service bridges may severely compromise the connectivity of complex networks, jeopardizing both the short-term fast deployment of emergency aids and the long-term ordinary life and growth of the social community. Reductions of functionality persisting over time may lead to unacceptable discomfort for the users. The infrastructure disservice can be quantified in monetary terms and user costs are associated with delay and detouring from the most convenient route due to the impossibility of transit over a bridge (Son and Sinha 1997, De Brito and Branco 1998, Thoft-Christensen 2009, Bai et al. 2013, Gervasio and da Silva 2013a, Twumasi-Boakye and Sobanjo 2017).

Transport authorities need appropriate criteria, methodologies and tools to quantitatively assist resource allocation and decision-making processes accounting for the uncertainties involved in the rate of occurrence of catastrophic events and in the large-scale consequences. Management strategies must face them with limited economical resources and without charging excessive expenditures on the users of the network. Cost models must be combined with suitable methods to assess the network performance. In turn, network performance must be linked to the seismic performance of individual bridges and related to the actual occurrence of disruptive seismic events in the area of the transportation system. In this context, risk-informed analysis tools consider many of the aforementioned aspects. Integrated frameworks for seismic risk assessment began to be developed in the late 90s, when casualties and economic losses related to several seismic events such as the 1994 Northridge earthquake and the 1995 Kobe earthquake emphasized the need for a performance-based approach (Günay and Mosalam 2013). The Pacific Earthquake Engineering Research (PEER) Center developed in 2003 a robust probabilistic framework for performance-based design (Porter 2003, Moehle and Dierlein 2004). In recent years, several research groups formalized seismic risk assessment methodologies to provide analytical frameworks aimed at evaluating probabilistic-based optimal planning strategies, such as seismic retrofit of bridges and road networks (Shiraki et al. 2007, Stergiou et al. 2010, Zhou et al. 2010, Dong et al. 2014a, Dong et al. 2014b, Mirzaei and Adey 2015).

Bridges are also particularly vulnerable to aging and structural deterioration due to environmental agents that can reduce over time their structural performance (Stein et al. 1999, Val and Stewart 2003, Biondini et al. 2004). Significant research advances have been accomplished for life-cycle design, assessment, and maintenance of structures and infrastructure systems (Biondini and Frangopol 2016, 2019). However, although the effects of degradation on structural performance have been extensively studied (Val and Melchers 1997, Enright and Frangopol 1998, Kassir and Ghosn 2002, Biondini et al. 2004, Biondini and Vergani 2015), their integration in life-cycle probabilistic seismic assessment and fragility frameworks has been deeply investigated only in recent years (Biondini et al. 2010, Ghosh and Padgett 2010, Akiyama et al. 2011, Biondini et al. 2011, Decò and Frangopol 2013, Biondini et al. 2014, Titi and Biondini 2015, Rao et al. 2017, Banerjee et al. 2019, Argyroudis et al. 2019, 2020, Capacci et al. 2020). The definition of an adequate trade-off between the inclusion of key aspects in an aggregated framework and the feasibility of simulation-based risk assessment for large road networks is not a trivial task. In fact, the complexity of models involved in describing different processes, such as bridge aging, seismic damage and its recovery as well as the consequences at the network scale, collides with the necessity of simulating a sufficient number of detrimental scenarios, without compromising the accuracy of the risk estimate (Yang and Frangopol 2020).

The use of resilience as an effective system performance indicator for life-cycle assessment of road networks has been discussed in Capacci and Biondini (2020). Further developments along these research lines are proposed in this paper to investigate the life-cycle seismic risk of bridges and road networks. To this aim, a comprehensive cost-based probabilistic framework for seismic risk assessment of spatially distributed bridge networks subjected to environmental aging is proposed. The seismic risk measure is formulated in terms of annual exceedance rate of a target threshold of user costs and the key factors having an influence on consequences for the users are taken into account along with the associated uncertainties.

In particular, Probabilistic Seismic Hazard Analysis (PSHA) and Monte Carlo simulation (MCS) based on Importance Sampling are exploited to reproduce the earthquake scenario in the region of interest in terms of seismic intensities at each bridge location. Damage scenarios and related traffic restrictions are obtained based on fragility curves associated with different limit states. Uncertainties on structural capacity deterioration due to aging is taken into account by time-variant parametric fragility curves and the restoration process of damaged individual bridges is considered based on probabilistic recovery curves. Finally, free-flow fastest-path traffic analysis is adopted to assess the loss of performance at network level and to quantify the user expenditures by suitable cost models.

The proposed approach is characterized by separate yet subsequent simulation steps: damage and recovery of individual bridges are obtained aggregating the information on seismic hazard and time-variant fragility curves, leading to network exposure assessment in terms of monetary losses based on traffic distribution analysis. The proposed framework relies on a free-flow traffic analysis based on the shortest-path assumption, neglecting traffic flow congestion in the process. This simplifying assumption aids the feasibility of the simulation process for real road networks, modeled by graphs with numerous nodes and road arcs and subjected to several damage scenarios of spatially distributed bridges. The methodology is applied to a real road network in the south of Lombardy region, Italy, reproducing the connectivity among four major cities, namely Lodi, Cremona, Crema, and Pavia, and the smaller neighboring municipalities. Despite the fact that the area of interest is characterized by low seismicity, the results allow to quantify the impact of environmental deterioration in increasing the seismic risk of the benchmark network. These results highlight the effectiveness of the proposed approach and emphasize the need for a life-cycle-oriented and risk-informed cost-based approach to support the decision making process of public authorities and bridge owners for optimal management, maintenance, repair, and upgrading of aging bridges and infrastructure transportation systems.

Impact analysis of roads networks

Road networks and graph theory

The performance of road networks can be evaluated based on traffic flows associated with different users of the transportation network. According to graph theory, a road network can be represented by a graph G=(V;E) defined in terms of the set of vertices V connected in pairs by road arcs collected in the set of edges E. In order to properly account for one-way roads, it is possible to make use of oriented graphs, in which any arc with origin vertex i and destination vertex j allows the transit from i to j but not from j to i. Consequently, two-way roads can be represented by a pair of edges connecting the same vertices with mutually opposite orientations. If N is the number of nodes in the network, the adjacency matrix $\mathbf{A}$ of G is defined as the N-dimension square matrix of the Boolean weights a_{ij}, such that a_{ij}=1 if node i and j are connected, 0 otherwise.

Vertices or nodes represent road intersections and all the points of the network that originate and attract trips, such as cities or other areas of interest (see for example Bocchini and Frangopol 2013). Origins and destinations of trips are associated with a subset of the vertices $Z \subseteq V$ and the traffic flows f_{od} can be suitably collected in the OD matrix, where each entry represents the trips generated from node o and attracted by node d.

Traffic assignment problem and demand properties

Traffic analysis consists in evaluating the distribution of the trips and travels within the transportation network given travel demand and network topology (LeBlanc et al. 1975). Typical mathematical models for traffic assignment can rely on free-flow analysis and congestion-based methods. In free-flow analysis, the traffic assignment problem is reduced to the definition of the shortest path between each OD pair. Along with the connectivity between every node pair in the graph provided by the adjacency matrix, each edge is characterized by a strictly positive weighting coefficient w_e. This analysis allows computing the optimal route from origin to destination that minimizes the sum of the weighting coefficients among any possible path across the road arcs. The weighting coefficients w_e can represent different edge parameters, such as their length or the travel time at free flow needed to cover the road arc. Traffic assignment is generally referred to shortest-path analysis in the former case and fastest-path analysis in the latter case. Mathematical techniques such as Dijkstra's algorithm (Dijkstra 1959) allow to efficiently compute the shortest path from a single node to all the other nodes in the network. On the other hand, congestion-based traffic assignment accounts for the actual traffic capacity of road segments. Most traffic analyses methods rely on the user-equilibrium assumption enforced by the Wardrop's gravitational model (Wardrop 1952), which is based on the principle that traffic flows are distributed in the network such that travel times on all routes are minimized. Additional insight can be found in Shinozuka et al. (2003), Dong et al. (2003), Bocchini and Frangopol (2011), Capacci et al. (2020). In the present work, free-flow analysis techniques have been preferred due to their lower computational cost and implementation effort. Users are assumed to travel along the fastest path to reach their destination and the selected route between each OD pair is computed based on the Dijkstra's algorithm. However, the theoretical definition of the framework is independent of the traffic assignment procedure.

Under operational conditions, traffic flows tend to be stationary and the definition of the OD matrix is obtained, for example, by surveys or traffic monitoring relying on sociological patterns and economical activities in the community. Such assumption of traffic demand inelasticity may be questioned in the aftermath of disastrous events, since disruptions in the transportation service prevent drivers to perform economically valuable activities such as working or shopping, changing trends and needs of road users (Shinozuka et al. 2003). In general, travellers can react to transport infrastructure failure in different ways, not only detouring failed links using the portion of the network in service, but also changing the travel modes and the destination of their planned activity, or even eliminating such activity suppressing the trips in the process (Erath et al. 2009). Drivers' reactions to infrastructure disservice would lead to a modification of the behaviour of the network users and, in turn, jeopardize system performance. Therefore, refined traffic analysis models should also take into account sociological aspects under emergency conditions that may lead not only to abrupt changes in users' planned trips, but also to irrational behaviour of drivers eventually exacerbated by the unavailability of traffic information (Feng et al. 2020). Nevertheless, there is also evidence that the prevailing behaviour of road users in emergency conditions is to modify routes and departing times, whilst the cancellation of the trip is a limited reaction (Giuliano and Golob 1998, Zhu and Levinson 2015, Jenelius and Mattsson 2015). In the present work, traffic demand is assumed to be inelastic, i.e. the occurrence of a seismic event does not lead to any variation of scheduled trips. Traffic demand is also assumed to be static, i.e. no daily or seasonal variations are taken into account.

Traffic limitations on damaged bridges

In the aftermath of extreme events such as earthquakes, bridges may undergo structural damage and managing agencies may need to apply suitable traffic restrictions proportional to the degree of damage. This would limit the traffic flows along damaged network components and may dramatically reduce the network performance. Traffic limitations on the b-th bridge are represented by a decision variable d_b. In the proposed framework, three progressively severe decision variables are taken into account, affecting two types of considered road users, namely light and heavy vehicles:

- No restrictions (d_b=0): both light and heavy vehicles are allowed to transit.
- Weight restriction (d_b=1): transit is forbidden to heavy vehicles.
- Closure (d_b=2): transit is forbidden to both road users.

The state of the network is represented by the vector of decision variables $\mathbf{d}=[d_1,d_2,\ldots, d_{n_b}]$, where n_b is the total number of bridges in the network.

In the representative graph of a road network, bridges may be modelled in two different ways:

1. They may be represented by two additional nodes corresponding to the extremes of the bridge and an additional edge included between the nodes.
2. They may be considered as properties of existing edges, i.e. their reduction of functionality affects the whole edge they are located on.

Whilst the first modelling technique is more accurate, the second approach is simpler and introduces some approximation depending on the possible functionality states of the bridges. Given the nature of the considered decision variables, the second modeling technique can be applied in the proposed framework without introducing any approximation. Therefore, bridges are assigned to their reference road arc that is eventually removed from the graph when traffic limitations prevent the transit of specific road users. In the proposed applications of the paper, the fastest path for each OD pair is computed given the traffic restriction combination **d**. Different modelling strategies could also be accommodated when considering other limitations of bridge traffic capacity with alternative flow analysis methods, such as speed limitation and lane restrictions along the damaged components.

Life-cycle costs

The occurrence of a seismic event may provoke economic losses related to physical damage of vulnerable facilities, to casualties and to functionality downtime. Cost components have been extensively studied in the context of life-cycle cost analysis (Chang and Shinozuka 1996, Frangopol 1999, Ozbay et al. 2004). They are generally distinguished in agency costs, user costs and third party costs (Ehlen 1999). Agency costs include all the expenditures incurred by the management body, such as repair, inspection and maintenance and have been widely examined (Frangopol et al. 2009, Kumar et al. 2009, Frangopol et al. 2017). Third party costs include all the costs that reflect on the whole social community and include cultural and environmental costs. User costs account for the discomforts to the users when the serviceability of the transportation system is temporarily impaired by bridge network restrictions (Chang and Shinozuka 1996). In particular, user costs may be equal or even greater than agency costs associated with ordinary maintenance (Koch et al. 2001, Kendall et al. 2008). Thus, user costs should be properly considered when dealing with loss quantification and risk assessment for road transportation networks. In the proposed framework, agency and third party costs are neglected, and user costs only are taken into account. User costs can be classified into three different components: driver delay cost (*DDC*), vehicle operating cost (*VOC*) and accident cost (*AC*) (see for example Gervásio and Da Silva 2013b, Zhang et al. 2013, Yavuz et al. 2017, Lemma et al. 2020). Each component can be related to the Total Travel Time (*TTT*) or to the Total Travel Distance (*TTD*) in the network, respectively defined as:

$$TTT(\mathbf{d}) = \sum_{o\in Z}\sum_{d\in Z} T_{od}(\mathbf{d})\cdot f_{od} \tag{1}$$

$$TTD(\mathbf{d}) = \sum_{o\in Z}\sum_{d\in Z} L_{od}(\mathbf{d})\cdot f_{od} \tag{2}$$

where T_{od} is the travel time associated with the fastest route from origin *o* to destination *d*, L_{od} is the travel distance associated with the fastest route from *o* to *d*, and f_{od} is the traffic flow from *o* to *d* in terms of vehicles per unit time.

DDC quantifies in monetary terms the value of time lost by the users due to detouring. With reference to the previously introduced notation, *DDC* is expressed as cost per unit time as follows:

$$DDC(\mathbf{d}) = (TTT(\mathbf{d}) - TTT_0)\cdot q_{DDC} \tag{3}$$

where TTT_0 is the total travel time associated with a full functionality state (i.e. $d_b = 0\ \forall\ b = 1,\dots,n_B$) and q_{DDC} is the estimated cost of time lost by each vehicle in the time unit. The traditional method for the evaluation of q_{DDC} is the so-called wage-rate method (Thoft-Christensen 2012), according to which q_{DDC} is based on a percentage of the mean hourly wage rate. Corotis (2007) points out that during long-term interruptions drivers tend to modify their behaviour and to relieve the discomfort. As a consequence, *DDC* does not derive directly from the productivity model. Despite of this drawback, data based on the wage rate method is exploited in the present study, due to the fact that only work travels are considered and that comparison among different scenarios is still reliable.

VOC represents the additional operational expenses associated with longer travel distances of vehicles. Consistently with *DDC*, it can be defined as follows:

$$VOC(\mathbf{d}) = (TTD(\mathbf{d}) - TTD_0) \cdot q_{VOC} \tag{4}$$

where TTD_0 is the total travel distance associated with a full functionality state and q_{VOC} is the unitary operating cost per vehicle in the road length unit. The cost parameter q_{VOC} includes all the costs related to the vehicle operations, mainly (Gervásio and da Silva 2013a): fuel and engine oil consumption, tyres consumption, maintenance and deterioration (represented by the depreciation of the vehicle). The value of q_{VOC} is strictly dependant on the type and on the category of the vehicle. It is generally obtained from technical data about vehicles and market surveys and an average regional value is finally adopted.

AC is associated with the increased estimated risk of vehicle accidents due to congestion. Due to the absence of congestion in the proposed traffic analysis method, the *AC* cost component is not considered in this study and only *DDC* and *VOC* are evaluated. In general, *DDC* is the dominant component of user costs (Kendall et al. 2008, Thoft-Christensen 2009).

The final cost per unit duration of the restriction scenario **d** is computed as:

$$\bar{u}(\mathbf{d}) = DDC(\mathbf{d}) + VOC(\mathbf{d}) \tag{5}$$

Finally, the comparison among different times requires the time-variant value of money to be taken into account. Thus, costs must be discounted to the same (initial) time:

$$u(\mathbf{d}) = \frac{\bar{u}(\mathbf{d})}{(1+\gamma)^{t_0}} \tag{6}$$

where γ is the monetary discount rate and t_0 is the occurrence time of the reference disruptive event. It is important to anticipate that the likelihood of occurrence of a specific bridge restriction scenario **d** depends on the time of occurrence t_0, since the reduction of structural capacity induced by environmental deterioration may affect the probability of occurrence of extensive damage and, in turn, of severe and prolonged traffic limitations.

Life-cycle seismic risk analysis of aging bridge networks

Probabilistic seismic hazard assessment of spatially distributed bridges

As first step in the risk assessment procedure, physical hazards capable of compromising the functionality of network must be identified. The occurrence rate of intense seismic events is represented by means of Probabilistic Seismic Hazard Analysis (PSHA) and the characteristics of relevant active tectonic faults are taken into account (McGuire 2007).

Due to the spatial distribution of the bridge sites with respect to the seismic source, both inter- and intra-event variability of seismic intensity must be taken into account by means of a suitable ground motion prediction equation (GMPE). The n_h random variables influencing the rate of occurrence and intensity of seismic events (e.g. moment magnitude, epicentre location, etc.) are collected in the vector of seismic hazard parameters $\mathbf{H}_h$ and seismic intensity is assumed to be a lognormal random variable conditioned on $\mathbf{H}_h$. Therefore, the seismic intensity scenario $\mathbf{I}$ is a multivariate random variable representing the seismic intensity at the site of the n_b vulnerable bridges within the network. The total probability theorem (Ang and Tang 2007) allows to define its probability density function (PDF) $f_{\mathbf{I}}(\mathbf{i})$:

$$f_{\mathbf{I}}(\mathbf{i}) = \int_{\mathfrak{R}^{n_h}} f_{\mathbf{I}|\boldsymbol{\eta}_\mathrm{h}}(\mathbf{i}|\boldsymbol{\eta}_\mathrm{h}) \cdot f_{\mathbf{H}_h}(\boldsymbol{\eta}_\mathrm{h}) \cdot d\boldsymbol{\eta}_\mathrm{h} \tag{7}$$

where $\mathbf{i}$ and $\boldsymbol{\eta}_\mathrm{h}$ are the vectors collecting the outcomes of $\mathbf{I}$ and $\mathbf{H}_h$, respectively.

The differential annual rate of exceedance of a given seismic intensity scenario is defined as follows:

$$|d\lambda(\mathbf{i})| = \left(\sum_k^{n_f} \nu_k\right) \cdot f_{\mathbf{I}}(\mathbf{i}) \cdot d\mathbf{i} \tag{8}$$

Where ν_k is the annual rate of earthquake occurrence for each of the k-th seismogenic sources in the region. It is worth noting that Eq. (8) holds if seismic events of given intensity are assumed to occur independently of each other, i.e. if they follow a Poisson process.

Time-variant fragility assessment of deteriorating RC bridges

Given the spatial distribution of seismic intensity, system vulnerability must be quantified to evaluate the damage state probability distribution following a hazardous event. In the present paper, bridge seismic capacity $I_{s,b}$ with respect to damage state s_b decreases during the bridge lifetime due to the effects aging and structural deterioration. However, it is worth noting that other sources of damage may induce an increase of seismic vulnerability over time, such as cumulative earthquake damage under successive earthquake shocks (Kumar et al. 2009, Gardoni and Kumar 2012, Ghosh et al. 2015, Ghosh and Panchireddi 2019) or different natural hazards, such as tsunamis (Akiyama et al. 2020). In reverse, the beneficial effects of maintenance and retrofit interventions improve bridge seismic capacity (Marì and Bairán 2008).

The marginal cumulative distribution function (CDF) of $I_{s,b}$, i.e. the fragility curve representing the probability of exceedance of s_b given the seismic intensity at the site of the b-th bridge i_b, can be expressed as a time-variant function:

$$P[S_b(t) \geq s_b | i_b] = F_{I_{s,b}(t)}(i_b) \qquad (9)$$

where S_b is a discrete univariate time-variant random variable representing the damage state of the b-th bridge in the network.

At single-bridge level, the difference between fragility curves associated with subsequent damages states provides the occurrence probability of damage state s_b:

$$P[S_b(t) = s_b | i_b] = F_{I_{s,b}(t)}(i_b) - F_{I_{s+1,b}(t)}(i_b) \qquad (10)$$

At system level, given the seismic intensity scenario **i,** the probability of intersection of the damage events related to the single bridges provides the probability of occurrence of a specific bridge damage combination **s**:

$$\{\mathbf{S}(t) = \mathbf{s} | \mathbf{i}\} = \{\cap_{b=1}^{n_b} [S_b(t) = s_b | i_b]\} \qquad (11)$$

where **S** is a discrete multivariate time-variant random variable representing the combination of bridge damage states. It is important to highlight that, together with the seismic intensity scenario **i**, the degree of correlation between seismic capacities of each pair of bridges in the network may have a relevant influence on the occurrence probability of the damage combination **s** (Capacci and Biondini 2018, 2019). Moreover, the effect of joint variations in time of seismic hazard, seismic fragility, and network exposure, may have a significant impact on the risk estimate (Zanini et al. 2017).

Life-cycle seismic risk of bridge networks

In the end of the risk assessment procedure, suitable performance indicators must be defined to quantify the operational disruption following the damage state combination **s** and evaluate the system exposure to the seismic event. If the occurrence of the earthquake at time t_0 had induced damage on the network components, infrastructure managers should apply specific limitations to the traffic flow. In addition, seismic damage to the b-th bridge requires repair interventions to be carried out and bridge downtime is related to the duration of the repair process (Padgett and DesRoches 2007, Mackie et al. 2009, Mackie 2010, Decò et al. 2013). The intervention starts at time $t_{i,b}$ and continues until full recovery time $t_{r,b}$, at which the pre-event condition is restored. The following recovery model $r_b = r_b(\tau) \in [0,1]$ is adopted over the bridge recovery time interval $\Delta t_{r,b} = t_{r,b} - t_{r,i}$ (Titi et al. 2015):

$$r_b(\tau) = \begin{cases} 0 & ,\tau \le 0 \\ \omega^{1-\rho}\tau^{\rho} & ,0 < \tau \le \omega \\ 1-(1-\omega)^{1-\rho}(1-\tau)^{\rho} & ,\omega < \tau \le 1 \\ 1 & ,\tau > 1 \end{cases} \tag{12}$$

where $\tau = \left(t - t_{i,b}\right)/\Delta t_{r,b} \in [0,1]$ is a normalized time variable. The shape of the recovery profile is defined by the parameters $\omega \in [0,1]$ and $\rho \geq 0$. The initial traffic limitations $d_b=k$ with $k>0$ are partially released through a progressively decreasing sequence of less severe restrictions $d_b=h$ with $h<k$, until $d_b=0$ at time $t_{r,b}$.

The user cost per unit duration of the restriction scenario over the time interval $\Delta t_h=t_h-t_0$ takes on the appearance of the following stepwise form:

$$u(t) = u_j = u(\mathbf{d}_j), \quad t_j \le t \le t_{j+1}\ \forall j \in [0, N_j] \tag{13}$$

where t_h is the horizon time, t_j is the time instant associated with a partial or total recovery time of a bridge in the network, N_j is the total number of time steps in the network recovery process. In other words, the user cost u_j at the j-th recovery step is associated to the traffic restriction combination $\mathbf{d}_j$. The cumulative user cost associated with event occurrence at time t_0 is given by the integral of the profile itself, that is:

$$C(t_0) = \int_{t_0}^{t_h} u(t_0, t)dt = \sum_{j=1}^{N_j} u_j \cdot \Delta t_j \tag{14}$$

where $\Delta t_j = t_{j+1} - t_j$ is the duration of the j-th recovery step of the network, as shown in Figure 1.

Due to the uncertainty in the recovery parameters ω and ρ, the user cost profile and the cumulative user cost are probabilistic components. Based on the total probability theorem, the time-variant CDF of the user cost measure conditional on a given seismic intensity scenario **i** can be defined as the weighted sum of the marginal user cost measure CDFs associated with a prescribed bridge damage combination **s** weighted by its probability of occurrence under given **i** (Capacci and Biondini 2020):

$$F_{C(t_0)|\mathbf{i}} = \sum_{k=1}^{n_f} F_{C|\mathbf{s}} \cdot P[\mathbf{S}(t) = \mathbf{s}|\mathbf{i}] \tag{15}$$

Given the Poissonian nature of the seismic hazard scenario, seismic risk can be quantified based on the annual rate of exceedance of a prescribed target of cumulative user cost as follows:

$$\nu_{C\geq c}(t_0) = \int_{\mathfrak{R}_+^{n_b}} F_{C(t_0)|\mathbf{i}}(c|\mathbf{i}) \cdot |d\lambda(\mathbf{i})| \tag{16}$$

The flow chart shown in Figure 2 illustrates the basic steps of the proposed life-cycle approach.

Exposure analysis of a case-study road network

Subnetwork in Lombardy Region (Italy)

The proposed methodology has been applied to a real road network in the north of Italy illustrated in Figure 3. The benchmark network is composed by 21 major bridges that connect four cities in the southern part of Lombardy region, namely Crema, Cremona, Lodi, and Pavia. The Italian road system classifies each road arc into highways, state roads, regional roads, provincial roads and municipal roads. Highways are generally managed by private agencies and have not been considered in this study. In order to focus the proposed study towards an application involving short-distance travels and commuting, the road network has been built considering all the other road categories, administrated by public agencies. Geographic data associated with roads has been manipulated by the software QGIS (QGIS 2016). Road arcs are available as line elements in different shapefiles associated with each road class (Open Data Portal Regione Lombardia, 2016). The network consists of 4331 nodes, 2043 primary roads (collecting state, regional and provincial roads) and 3500 secondary or municipal roads. The arc travel times have been computed based on the ratio between road category free-flow speed and arc length. Speed has been set equal to 110 km/h for primary roads and to 60 km/h for secondary roads. It is worth noting that the graph representative of the road network has been built by splitting out line elements at their intersection points. Based on available data for graph generation, it is not possible to identify overpasses or underpasses that have been taken into account as fictitious road intersections. Consequently, this lack of data may involve overestimation of network connectivity and approximation of user costs. For example, when bridges are in pristine conditions, the computed fastest route may be faster than the actual fastest route. Thus, travel time may be underestimated and DDC may be overestimated. Contrary, when bridges are damaged, the computed fastest path may be faster than the actual fastest route. Thus, both additional travel time and DDC may be underestimated.

The inelastic traffic demand adopted in this study has been retrieved from the OD matrices available from the Open Data Portal, Regione Lombardia (2016). These were obtained by interpolating the results of transport models, online or physical surveys and previous studies on the traffic demand. The OD matrix for light traffic of the entire Lombardy region is referred to 1450 zones mostly coinciding with the individual municipalities, with the exception of few wider cities that are further divided in subzones. OD matrices for heavy traffic are referred to 437 zones, mostly obtained by merging the light traffic ones. In particular, the selected subnetwork of interest is characterized by 93 and 32 zones for light and heavy vehicles, respectively.

OD data are available for different time slots and they have been aggregated to obtain daily traffic flows. Heavy traffic data is available for three vehicle categories (distinguished by their mass). For light vehicles, traffic flows are available for five travel types (work, study, occasional, business, home return) and eight modes (car-driver, car-passenger, public transport-road, public transport-railways, motorbike, bike, on foot, other). In this study, all heavy vehicles have been taken into account, whilst only work travels by car (both driver and passenger) and by motorbike have been considered. Traffic zones and daily trip densities from Origin municipalities are shown in Figure 4, summarized in terms of travel types for light traffic and vehicle categories for heavy traffic. In order to generate the OD pairs within the road graph, travel demands have been assigned to the closest node to the zone centroid. The dimensions of circles representing trip densities are scaled with respect to the largest density in the region for each traffic category. In particular, heavy traffic demand tends to be much smaller compared to light traffic, mostly because of the tendency of heavy vehicles to cover longer distances and, in turn, use highways to reach their destination.

Twenty-one vulnerable bridges have been considered in the proposed application. These are located along the routes of regional interest according to the Regional Mobility and Transportation Program (Regione Lombardia 2016) approved by the regional council in 2016. Locations and labelling of each bridge are illustrated in Figure 5, where the thick lines represent the routes of regional interest. This is only a fraction of the total number of bridges in the area of interest, for which data in terms of geographical location and structural typology is available. Bridge #13 results to be particularly critical, since it belongs to the only road segment connecting the south-west zone with the rest of the network. Actually, detours are available on the roads of the adjacent Emilia-Romagna region, that have not been modelled in the proposed application due to unavailability of data. Both slight or extensive damage to bridge #13 would lead to theoretically infinite travel times and user costs due to the fictitious isolation of few traffic zones. To avoid this modelling issue, costs related to the isolated traffic zones due to the closure of bridge #13 have been fixed to a predetermined value. *VOC* has been assumed to be zero and *DDC* has been computed according to a fictitious delay of 8 hours, corresponding to a typical workday. Further details on the so-called cut links may be found in Jenelius et al. (2006), Jenelius (2010), Rupi et al. (2015).

User cost analysis

Cost parameters have been obtained from different technical reports. In particular, the value of unit time for light vehicles has been set to 25.78 €/(vehicle · hour) and has been adapted from the results of the Harmonizing European Approaches for Transport Costing (HEATCO) report (Odgaard et al. 2005), which are based on the wage rate method. The same source has been exploited for the unit operating cost of light vehicles, equal to 0.22 €/(vehicle · km). The value of unit time for heavy vehicles has been retrieved from the Comité National Routier report about road freight transport in Italy (Comité National Routier 2017) and is equal to 29.76 €/(vehicle · hour). Unit operating cost for heavy vehicles has been obtained from the COMPETE final report (Maibach et al. 2006) by averaging the value for light and heavy duty freight vehicles and is equal to 0.85 €/(vehicle · km). For the discount factor, the range 2-8% is usually considered for industrialized countries like Italy (Santander and Sanchez-Silva 2008). Based on data provided by the Italian Ministry of Economy and Finance (MEF 2018), a value γ=2% has been adopted in this paper. Additional information about the calibration of the discount factor can be found in Rackwitz et al. (2005) and Rackwitz (2006), among others.

In order to quantify the relative importance of the bridges in the network in terms of user losses, network exposure in terms of user costs has been examined by closing one bridge at a time and computing *TTT*, *TTD*, *DDC* and *VOC* according to Eqs. (1) to (4). Since no congestion is considered in the framework, it is possible to assume that one travel equals one vehicle in the computation of *DDC*. The same cannot be done for *VOC* and car passengers have been excluded from its evaluation. A total number of n_b=21 scenarios has been studied. The *i*-th scenario is such that d_b=2 for b=i and d_b=0 otherwise. Results are shown in Figure 6, where daily *DDC* and *VOC* due to the isolated closure of each bridge are shown. Bridge #13 is the most critical one, whilst the isolated closure of some others, such as bridges #17 or #18, has a slightly perceivable impact on the traffic distribution. Results also highlight that daily user costs are much higher for light vehicles than heavy ones. Concerning with cost items, *DDC* is confirmed to be the dominant one, whilst *VOC* was proved to surely an impactful cost element in one case, even higher than *DDC* for Bridge #7. In fact, on the one hand, distance increase rate due to detour tends to be about two orders of magnitude greater than the travel time increase rate. On the other hand, unit cost parameters for *VOC* are about two orders of magnitude lower than *DDC* ones. In particular, *DDC* tends to be predominant when fastest paths cover short road arcs at low free-flow speed and, conversely, large *VOC* derives from paths over high-speed long roads.

A similar approach has been adopted to assess the relative importance of three routes of regional interest. Three network states were defined such that d_b=2 if the *b*-th bridge belongs to the examined route and d_b = 0 otherwise. Note that 8 bridges belong to route 1, 3 to route 2 and 5 to route 3, whilst the other 5 bridges do not belong to any route in particular and have been therefore assumed to work at full functionality (see Figure 5). Results are reported in Table 1 and represented in Figure 7. The highest user costs are obtained along Route 3, connecting the cities of Pavia and Cremona. These are one order of magnitude greater than the ones associated with Route 1 (Pavia-Crema), and no significant loss is associated with the bridges on Route 2 (Cremona-Crema). In terms of light/heavy vehicles and *DDC*/*VOC* cost items, Figure 7 confirms the same trends highlighted for the case of isolated bridge closure. Under the constitutive assumption in the proposed approach that users follow the fastest available path, traffic restrictions may force them to follow a more time-consuming route along secondary roads yet covering shorter travel distances. In this case, negative yet relatively small values of *VOC* may arise in the cost cumulation process.

Seismic risk assessment of the case-study road network

Seismic hazard of the investigated area

The proposed seismic risk assessment framework has been applied to the investigated bridge network. The area is characterized by a low level of seismic hazard. According to the seismic hazard maps provided by the Italian Institute of Geophysics and Volcanology (INGV), the area falls into the medium-low seismicity category (Zone 3 out of 4). As a general reference, the values of peak ground acceleration expected to occur with 10% probability in 50 years range between 0.05g and 0.10g.

The complex distribution of epicenters of historical earthquakes has moved the common practice towards the use of area seismic sources (Barani et al. 2009). The seismogenic zonation ZS9 for Italy (Meletti et al. 2008) has been adopted in this study and Figure 8 shows the considered area sources in proximity of the bridge network (namely Zones 906, 907, 911 and 913), whose centroids are less than 50 km from the closest bridge. The probabilistic model for moment magnitude occurrence is characterized by truncated Gutenberg-Richter distribution (Gutenberg and Richter 1944) and the values of shape parameter b, minimum and maximum magnitudes $m_{\min}$ and $m_{\max}$ and annual recurrence rate $\nu_{m\geq m_{\min}}$ for the areas of interest are reported in Table 2.

The ground motion prediction model derived from the Italian strong motion database has been adopted (Bindi et al. 2011), which can account for different predominant faulting mechanisms and provides information on within- and between-event variability of the ground motion. In accordance with Eqs. (7) and (8), seismic intensities at the bridge sites $\mathbf{i}$ in terms of spectral accelerations at 1 second $S_a(T=1\text{s})$ have been simulated based on the adopted attenuation model by generating 10^5 samples of epicenter locations (see small dots in Figure 8), moment magnitudes and residuals. The computational effort was reduced by the adoption of a simulation framework based on Importance Sampling (Jayaram and Baker 2010). In order to increase the likelihood of simulating moment magnitudes leading to a sufficient number of seismic intensity maps that may induce bridge damage, a truncated Gutenberg-Richter distribution with shape parameter b=–1.0 has been selected. In this way, the number of samples leading to severe damage combinations is increased without compromising the accuracy of the risk estimate. Figure 9 shows the original truncated Gutenberg-Richter cumulative distributions for each seismogenic zone and the one adopted for the simulation.

Seismic vulnerability of aging bridges

At the system level, seismic vulnerability of individual bridges can be expressed in probabilistic terms by means of fragility curves, which represent the exceedance probability of a prescribed limit state s_b for a given seismic intensity i_b. Due to the considerable number of bridges in real road networks, transport agencies must face with the many economic and logistic difficulties in acquiring detailed data and calibrate refined models for each bridge in the network. Therefore, parametric and taxonomic fragility assessment methods are often adopted for risk assessment of systems of structures, such as infrastructure networks (Karim and Yamazaki 2003, Mackie and Stojadinovic 2007, Tsionis and Fardis 2014, Shekhar and Ghosh 2020). Fragility curves for pristine bridges have been retrieved from the FEMA Multi-Hazard Loss Estimation Methodology HAZUS – MH 2.1 (Mander 1999, HAZUS 2012). HAZUS fragility curves rely on lognormal models in terms of spectral accelerations at reference period of 1 second $S_a(T=1\text{s})$. Fragility curves due to ground shaking were available for 28 classes of bridges and 4 limit states (slight, moderate, extensive and collapse). No restriction (d_b=0) has been applied on undamaged (s_b=0) bridges. Slight (s_b=1) and extensive (s_b=2) damage states have been associated with the closure to heavy (d_b=1) and both light and heavy traffic (d_b=2), respectively. Each bridge has been classified according to HAZUS taxonomy and assigned to one of HAZUS structural categories based on available information, as reported in Table 3. The HAZUS framework may also accommodate via multiplicative coefficients information on geometry and mechanical parameters such as natural periods, deck skewness and tri-dimensional arch-effect.

With reference to Eq. (9), time-variant lognormal fragility curves are assumed and expressed in analytical terms as follows:

$$P[S_b(t) \geq s_b | i_b] = \Phi\left(\frac{\ln i_b - \lambda_{s,b}(t)}{\zeta_{s,b}}\right) \tag{17}$$

where Φ denotes the standard normal CDF, whilst $\lambda_{s,b}$ and $\zeta_{s,b}$ are the constitutive statistical parameters of the lognormal distribution representing central value and dispersion for limit state s_b. In particular, the dispersion has been assumed to be $\zeta_{s,b} = 0.6$ for any bridge, damage state and time of earthquake occurrence. Aging effects have been considered by reducing the median values of the fragility curves. A parabolic degradation law has been adopted based on Ghosh and Padgett (2010) and it can be expressed in terms of a corrosion rate parameter α as follows:

$$\lambda_{s,b}(t) = \bar{\lambda}_{s,b} \cdot (1 - \alpha t^2) \tag{18}$$

where $\bar{\lambda}_{s,b}$ is the logarithm of the median bridge seismic capacity in pristine conditions. The reduction in time of the median fragility value is dependent on both the bridge characteristics and type of deterioration mechanism. In the proposed application, the corrosion rate parameter has been set to α=5.1·10^{-5} 1/years^2 in order to enforce a 25% reduction after 70 years of the median seismic capacity for any bridge and limit state (Decò and Frangopol 2013, Dong et al. 2014b). Figure 10 graphically resumes the procedure to associate the time-variant fragility curves for each vulnerable aging bridge in the network.

Based on the time-variant statistical model representative of network seismic vulnerability, Monte Carlo simulation can be exploited to generate at n_t discrete time instants a set of 10^5 realizations of seismic capacities to both slight and extensive damage associated with each bridge. Given the realizations of seismic scenarios in terms of seismic intensities **i** at each bridge location, 10^5 damage scenarios **s** have been obtained based on Eq. (11) at each occurrence time of the seismic event t_0, namely from 0 to 100 years every 10 years. Bridges have been assumed to be in pristine conditions at t_0=0. The empirical estimate of the limit state exceedance is shown in Figure 11. The combination of regional seismic hazard and bridge seismic vulnerability generally results in higher occurrence of the slight damage state with respect to the extensive damage one. Moreover, the progressively decaying structural capacity of aging bridges substantially increases the occurrence frequencies of both damage states. Bridge structural typologies and their epicenter distance may have a considerable effect on the likelihood of occurrence of damage at different ages of the infrastructure.

Damage and recovery of network functionality

In order to account for the uncertainties in the network restoration process, described by Equation (12), random variables have been adopted to model the governing parameters of bridge structural recovery, namely shape parameters ω and ρ , idle time $t_{i,b}$ and repair completion time $t_{r,b}$. The statistical parameters of each distribution are shown in Table 4. In particular, ω has been modelled as a standard Beta distribution, whilst ρ, $t_{i,b}$ and $t_{r,b}$ have been assumed to be uniformly distributed (Capacci and Biondini 2020).

Based on the analytical recovery model of structural capacity from a given bridge damage state s_b, it has been possible to simulate the network recovery process in terms of decision variables **d** at discrete recovery time steps t_j, allowing to statistically evaluate the user costs profile and its cumulative value. For each of the $10^5 \times n_t$ realizations of network damage states, the network recovery profiles have been computed by sampling the associated random variables and fastest path analysis allowed to retrieve the daily user cost profiles $u(t)$ and the associated cumulative user costs $C(t_0)$ according to Equations (13) and (14), respectively.

Time-variant exceedance rate of user costs threshold

Figure 12 illustrates the results of the simulation in terms of user costs at different time instants. Each dot represents a sample value of the user cost for a given earthquake occurrence time versus the moment magnitude of the causative seismic scenario. The adoption of Importance Sampling for the seismic scenario generation allows to produce a relatively large number of high-magnitude samples, which may induce significant widespread damage leading to larger network exposure.

For each time t_0, the annual rate of exceedance of a user cost threshold equal to 1M € has been computed according to Equation (16) based on the results of the simulation. Table 5 resumes the values of the risk measure for different occurrence times. In the first

50 years no substantial increase of risk is observed, whilst the value at 60 years is about four to five times larger than the pristine condition. After 90 years, seismic risk has increased of more than one order of magnitude. Figure 13 represents the time-variant seismic risk measures associated with the total user costs and its disaggregation into the components associated with driver delays and vehicle operations. As anticipated by the exposure analysis, risk associated to *DDC* is greater yet not dominant over *VOC*.

Finally, Figure 14 shows the seismic risk measure disaggregated into cost items associated with light and heavy vehicles. Seismic risk for light vehicles is dominant in the first 50 years. Such trend tends to reverse under severe environmental deterioration, especially due to the progressive increase of slight damage occurrence probability.

Effects of correlation among bridge deterioration patterns

Aging and deterioration of bridges are strongly influenced by the bridge characteristics, such as year of construction, volume of traffic and type of structural system (Kim and Yoon 2010). Moreover, external factors such as presence of water or diffusion of aggressive chemical agents such as chlorides (Marsh and Frangopol 2008, Biondini and Frangopol 2008, Titi and Biondini 2016) may have severe detrimental effects in triggering and exacerbating the degradation process. Therefore, knowledge of the bridge exposure conditions is of fundamental importance for the characterization of the aging phenomenon, allowing for the calibration of refined models reproducing the actual loss of seismic structural capacity (Choe et al. 2009, Zhong et al. 2012, Shekhar et al. 2018). Nearby bridges are likely to have similar exposure conditions and to undergo similar deterioration processes, whilst far away bridges may show significant differences in the aging process. Based on such considerations, spatial interpolation techniques such as kriging procedures may be adopted when information about a subset of bridges in a larger portfolio is available from in-field inspection or monitoring (Rokneddin et al. 2014, Ghosh et al. 2014).

For the case study subnetwork in Lombardy Region presented in the previous section, the same degradation law has been enforced for all bridges, thus assuming perfect correlation among deterioration patterns. In order to investigate the influence of such correlation on the life-cycle risk estimate, a different corrosion rate parameter α_b has been considered for each of the n_b=21 bridges and each parameter has been modelled as a random variable A_b. By denoting ρ_{ij} the correlation coefficient between the aging rates A_i and A_j of bridges i and j, three different cases have been analyzed: null correlation with

ρ_{ij}=0, perfect correlation with ρ_{ij}=1, and distance-based correlation to reproduce similar deterioration patterns for nearby bridges with:

$$\rho_{ij} = \begin{cases} e^{-d_{ij}/\bar{d}} & \text{for } d_{ij} < \bar{d} \\ 0 & \text{for } d_{ij} \geq \bar{d} \end{cases} \tag{19}$$

where d_{ij} is the distance between bridges i and j and $\bar{d} = 25$ km. It is worth noting that the minimum and maximum distances between two bridges are 0.07 and 68 km, respectively, and that the reference distance $\bar{d}$ has been set to obtain a mean value of the correlation coefficients $\bar{\rho} \approx 0.50$. A marginal normal truncated PDF has been assumed for the random variables A_b. The mean value corresponds to the nominal corrosion rate parameter adopted in the previous analysis, i.e. 25% reduction of the median fragility value in 70 years. The coefficient of variation is assumed to be equal to 0.17. Finally, the lower the upper bounds correspond to 15% and 35% reduction of the median fragility value in 70 years, respectively.

Monte Carlo simulation for the corrosion rate parameters has been integrated into the previously presented framework to compare the life-cycle cost-based seismic risk associated with the three different correlation cases. In accordance with the proposed framework, seismic risk has been evaluated in terms of annual rate of exceedance of a cost threshold equal to 1M €. However, since results from the previous analysis have shown strong accordance between the DDC and VOC cost components, DDC only is considered as user cost in the comparison of the three investigated cases. Results are presented in Figure 15 for six occurrence times of the seismic event t_0, namely from 0 to 100 years every 20 years.

As expected, seismic risk increases with the correlation level, although differences are observable only after severe deterioration takes place, i.e. t_0 > 40 years. In particular, the annual rate of exceedance of the cost threshold associated with the null-correlation scenario is sensibly lower than the one associated with the two other scenarios because of the higher number of possible damage scenarios. Increase of seismic risk over time due to bridge deterioration is more pronounced for the distance-based and perfect correlation, whilst the difference among such two scenarios is reduced for t_0 > 80 years due to the relevant effect of corrosion, which strongly compromises bridge seismic capacities regardless of the correlation law.

Conclusions

Bridges can be severely damaged by seismic events and traffic restrictions are applied in the aftermath of earthquakes by transport authorities and road network operators to guarantee the users' safety in emergency conditions, temporarily compromising the functionality of damaged transportation networks. Road users can be strongly affected by serviceability downtime and traffic flow discomforts, leading to financial losses to be quantified in monetary terms. Nonetheless, aging effects are likely to exacerbate the consequences of an earthquake, reducing over time the capacity of bridge structures to sustain the detrimental effect of hazardous events. To face this problem, an integrated procedure for cost-based risk assessment has been proposed to quantify the impact of spatially distributed seismic events on aging bridge networks. In particular, seismic risk of the aging network is formulated in analytical form in terms of annual rate of exceedance of a target user cost threshold.

The proposed analytical framework is established based on the definition of a risk metric that comprehensively aggregates all the uncertainties involved in life-cycle seismic assessment. Starting from the probabilistic model, each basic component is numerically simulated to obtain a quantitative estimate of cost-based life-cycle seismic risk measure. Given the active tectonic faults in the area, seismic intensity scenarios are first simulated via advanced sampling techniques. Then, fragility curves are calibrated to simulate time-variant bridge seismic capacities, damage occurrence and the associated post-earthquake traffic restrictions. Probabilistic recovery profiles allow to retrieve the evolution of network functionality during the repair process. Finally, cumulative user costs are quantified based on the results of free-flow fastest path analysis, which reproduces the network performance decay in terms of travel delays and detour distances.

The framework is applied to a real road network in the south of Lombardy region, Italy. Bridge traffic limitations might be either critical or irrelevant on user costs depending on road network topology and Origin-Destination travel demands. Regardless of the structural capacity of vulnerable elements and the regional seismic hazard, exposure analysis under prescribed combinations of restrictions allows to identify the most relevant bridges within the network and the most impactful cost items in terms of potential economic losses. In the proposed risk-based framework, traffic restrictions actually derive from the combination of hazard and vulnerability information. Large seismic risk indicates how widespread damage of vulnerable bridges can have severe consequences on the economic operations of road users. Moreover, the progressive decay of bridge structural capacity induced by environmental aging plays an important detrimental role in exacerbating seismic vulnerability, increasing the risk estimate of more than one order of magnitude over 90 years despite of the relatively low seismic hazard in the network area. Even though bridge degradation and recovery have been reproduced based on the few available information, such results may be useful to assist ex-ante planning and decision-making by transport authorities and to develop reliable risk mitigation strategies, incorporating the economic consequences for road users based on a life-cycle perspective and preserving the fundamental role of road connectivity in sustainability and development of urban and rural communities. Further research efforts should be devoted at gathering new data from existing structures for calibration and validation of the degradation and recovery models. Along this line, further analysis has proved that correlation among the deterioration patterns of different bridges may have relevant effects on the life-cycle risk estimate.

It is worth noting that the framework is able to accommodate different analysis methods for each risk component. For example, congestion-based strategies with dynamic elastic traffic demand may be used in place of the adopted fastest path analysis with static inelastic users' Origin-Destination travel patterns. In this context, further research should aim at investigating the actual relevance of the traffic analysis technique in order to individuate a proper trade-off between accuracy and computational efficiency. Moreover, in order to improve such trade-off, sensitivity analyses should be carried out with respect to different parameters of the simulation (e.g. sample size, sampling distribution). Network exposure should be represented by comprehensive monetary metrics including not only user costs, but also management expenditures and social losses. The proposed framework not only can easily incorporate additional cost items such as agency maintenance costs, but can also be extended to measure seismic risk in terms of non-monetary performance indicators, such as redundancy, robustness, and resilience of spatially distributed structural systems.

References

Akiyama, M., Frangopol, D., Matsuzaki, H., 2011. Life-cycle reliability of RC bridge piers under seismic and airborne chloride hazards. *Earthquake Engineering and Structural Dynamics, 40*(15), 1671-1687.

Akiyama, M.; Frangopol, D. M., Ishibashi, H., 2020. Toward Life-Cycle Reliability-, Risk- and Resilience-Based Design and Assessment of Bridges and Bridge Networks

Under Independent and Interacting Hazards: Emphasis on Earthquake, Tsunami and Corrosion. *Structure and Infrastructure Engineering: Maintenance, Management, Life-Cycle Design and Performance 16*(1): 26-50.

Ang, A., Tang, W., 2007. *Probability concepts in engineering: Emphasis on applications to civil and environmental engineering. Volume I.* (2nd Ed.). John Wiley & Sons.

Argyroudis, S., Mitoulis, M., Winter, M. G., Kanya, A. M., 2019. Fragility of transport assets exposed to multiple hazards: State-of-the-art review toward infrastructural resilience. *Reliability Engineering and System Safety 191*: 106567

Argyroudis, S., Mitoulis, M., Hofer, L., Zanini, M. A., Tubaldi, E., Frangopol, D.M., 2020. Resilience assessment framework for critical infrastructure in a multi-hazard environment: Case study on transport assets. *Science of the Total Environment 714*: 136854.

Bai, Q., Labi, S., Sinha, K., Thompson, P., 2013. Bridge user cost estimation–A synthesis of existing methods and addressing the issues of multiple counting, workzones and traffic capacity limitation. *Structure and Infrastructure Engineering, 9*(9), 849-859.

Banerjee, S., Shinozuka, M., 2008. Experimental verification of bridge seismic damage states quantified by calibrating analytical models with empirical field data. *Earthquake Engineering and Engineering Vibration, 7*(4), 383-393.

Banerjee, S., Vishwanath, B., Devendiran, D., 2019. Multihazard resilience of highway bridges and bridge networks: a review. *Structure and Infrastructure Engineering 15*(12): 1694-1714.

Barani, S., Spallarossa, D., Bazzurro, P., 2009. Disaggregation of probabilistic ground-motion Hazard in Italy. *Bulletin of the Seismological Society of America, 99*(5), 2638-2661.

Bindi, D., Pacor, F., Luzi, L., Puglia, R., Massa, M., Ameri, G., Paolucci, R., 2011. Ground motion prediction equations derived from the Italian strong motion database. *Bulletin of Earthquake Engineering, 9*(6), 1899-1920.

Biondini F., Bontempi F., Frangopol D.M., Malerba P.G. 2004. Cellular automata approach to durability analysis of concrete structures in aggressive environments. *Journal of Structural Engineering*, ASCE, 130(11), 1724-1737.

Biondini, F., Camnasio, E., Palermo, A., 2010. Seismic performance of concrete structures in aggressive environments, *Second International Symposium on Life-Cycle Civil Engineering* (IALCCE 2010), Taipei, Taiwan, October 27-31, 2010. In: S.-S. Chen, A.-H. Ang, D.M. Frangopol (Eds.), *Life-Cycle of Civil Engineering Systems*, Taiwan Tech, National Taiwan University of Science and Technology, Taiwan.

Biondini, F., Camnasio, E., Palermo, A., 2014. Lifetime seismic performance of concrete bridges exposed to corrosion. *Structure and Infrastructure Engineering, 10*(7), 880-900.

Biondini, F., Frangopol, D. M., 2008. Probabilistic limit analysis and lifetime prediction of concrete structures. *Structure and Infrastructure Engineering 4*(5): 399-412.

Biondini, F., Frangopol, D. M., 2016. Life-cycle performance of deteriorating structural systems under uncertainty: Review. *Journal of Structural Engineering, 142*(9), F4016001.

Biondini, F., Frangopol, D.M. (Eds.), 2019. *Life-Cycle Design, Assessment and Maintenance of Structures and Infrastructure Systems*, American Society of Civil Engineers (ASCE), Reston, VA, USA.

Biondini, F., Palermo A., Toniolo, G. 2011. Seismic performance of concrete structures exposed to corrosion: Case studies of low-rise precast buildings, *Structure and Infrastructure Engineering 7*(1–2): 109-119.

Biondini, F., Vergani, M., 2015. Deteriorating beam finite element for nonlinear analysis of concrete structures under corrosion. *Structure and Infrastructure Engineering, 11*(4), 519-532.

Bocchini, P., Frangopol, D. M., 2011. A stochastic computational framework for the joint transportation network fragility analysis and traffic flow distribution under extreme events. *Probabilistic Engineering Mechanics, 26*(2), 182-193.

Bocchini, P., Frangopol, D.M., 2013. Connectivity-based optimal scheduling for maintenance of bridge networks. *Journal of Engineering Mechanics 139*(6): 760-769.

Capacci, L., Biondini, F., 2018. Life-cycle seismic resilience of aging bridges and road networks considering bridge capacity correlation. *9th International Conference on Bridge Maintenance, Safety and Management (IABMAS 2018)*, Melbourne, Australia, July 9-13, 2018.

Capacci, L., Biondini, F., 2019. Seismic resilience of bridges and road networks under climate change. *2019 IABSE Congress New York City, The Evolving Metropolis.*

Capacci, L., Biondini, F., 2020. Probabilistic life-cycle seismic resilience assessment of aging bridge networks considering infrastructure upgrading. *Structure and Infrastructure Engineering*, *16*(4), 659-675.

Capacci, L., Biondini, F., Titi, A., 2020. Lifetime seismic resilience of aging bridges and road networks. *Structure and Infrastructure Engineering, 16*(2), 266-286.

Carturan, F., Pellegrino, C., Rossi, R., Gastaldi, M., Modena, C., 2013. An integrated procedure for management of bridge networks in seismic areas. *Bulletin of Earthquake Engineering*, 11(2), 543–559.

Chang, S., Shinozuka, M., 1996. Life-cycle cost analysis with natural hazard risk. *Journal of Infrastructure Systems, 2*(3), 118-126.

Choe, D. E., Gardoni, P., Rosowsky, D., Haukaas, T., 2009. Seismic fragility estimates for reinforced concrete bridges subject to corrosion. *Structural Safety 31*(4): 275-283.

Corotis, R., 2007. Highway user travel time evaluation. *Journal of Transportation Engineering, 133*(12), 663-669.

Comité National Routier, 2017. *Le transport routier de marchandises en Italie – Étude 2017*, CNR European Studies. <http://www.cnr.fr/Publications-CNR/Le-TRM-Italien-2017>. Last access: March 1st, 2020.

De Brito, J., Branco, F., 1998. Road bridges functional failure costs and benefits. *Canadian Journal of Civil Engineering, 25*(2), 261-270.

Decò, A., Frangopol, D. M., 2013. Life-cycle risk assessment of spatially distributed aging bridges under seismic and traffic hazards. *Earthquake Spectra, 29*(1), 127-153.

Decò, A., Bocchini, P., Frangopol, D.M., 2013. A probabilistic approach for the prediction of seismic resilience of bridges. *Earthquake Engineering and Structural Dynamics 42*(10), 1469-1487.

Dijkstra, E., 1959. A note on two problems in connexion with graphs. *Numerische Mathematik, 1*(1), 269-271.

Dong, Y., Frangopol, D. M., Saydam, D., 2014a. Pre-earthquake multi-objective probabilistic retrofit optimization of bridge networks based on sustainability. *Journal of Bridge Engineering, 19*(6), 040114018.

Dong, Y., Frangopol, D. M., Saydam, D., 2014b. Sustainability of highway bridge networks under seismic hazard. *Journal of Earthquake Engineering, 18*(1), 41-66.

Ehlen, M., 1999. Life-cycle costs of fiber-reinforced-polymer bridge decks. *Journal of Materials in Civil Engineering, 11*(3), 224-230.

Enright, M., Frangopol, D.M., 1998. Probabilistic analysis of resistance degradation of reinforced concrete bridge beams under corrosion. *Engineering Structures, 20*(11), 960-971.

Erath, A., Birdsall, J., Axhausen, K., Hajdin, R., 2009. Vulnerability assessment methodology for swiss road network. *Transportation Research Record 2137*(1), 118-126.

Feng, K., Li, Q., Ellingwood, B., 2020. Post-earthquake modelling of transportation networks using an agent-based model. *Structure and Infrastructure Engineering*, 1-15. DOI: 10.1080/15732479.2020.1713170.

Frangopol, D. M., 1999. *Life-cycle cost analysis for bridges.* In: *Bridge Safety and Reliability* (D. M. Frangopol, ed.)*,* ASCE, Reston, VA, pp. 210–236.

Frangopol, D.M., Strauss, A., Bergmeister, K., 2009. Lifetime cost optimization of structures by a combined condition-reliability approach. *Engineering Structures, 31*(7), 1572-1580.

Frangopol, D. M., Dong, Y., Sabatino, S., 2017. Bridge life-cycle performance and cost: analysis, prediction, optimisation and decision-making. *Structure and Infrastructure Engineering, 13*(10), 1239-1257.

Gardoni, P., Kumar, R., 2012. Modeling structural degradation of RC bridge columns subjected to earthquakes and their fragility estimates. *Journal of Structural Engineering*, 138(1), 42-51.

Gervásio, H., da Silva, L., 2013a. Life-cycle social analysis of motorway bridges. *Structure and Infrastructure Engineering, 9*(10), 1019-1039.

Gervásio, H., da Silva, L., 2013b. A design approach for sustainable bridges – Part 1:Methodology. *Proceedings of the Institution of Civil Engineers: Engineering Sustainability 166*(4): 191-200

Ghosh, J., Padgett, J., 2010. Aging considerations in the development of time-dependent seismic fragility curves. *Journal of Structural Engineering, 136*(12), 1497-1511.

Ghosh, J., Rokneddin, K., Padgett, J. E., Dueñas-Osorio, L., 2014. Seismic Reliability Assessment of Aging Highway Bridge Networks with Field Instrumentation Data and Correlated Failures, I: Methodology. *Earthquake Spectra 30*(2): 795 817.

Ghosh, J., Padgett, J., Sánchez-Silva, M., 2015. Seismic damage accumulation in highway bridges in earthquake-prone regions. *Earthquake Spectra*, 31(1), 115-135.

Ghosh, J., Panchireddi, B., 2019. Cumulative vulnerability assessment of highway bridges considering corrosion deterioration and repeated earthquake events. *Bulletin of Earthquake Engineering*, 17(3), 1603-1638.

Giuliano, G., Golob, J., 1998. Impacts of the Northridge Earthquake on Transit and Highway Use. *Journal of Transportation and Statistics, 1*(2), 1-20.

Günay, S., Mosalam, K., 2013. PEER performance-based earthquake engineering methodology, revisited. *Journal of Earthquake Engineering, 17*(6), 829-858.

Gutenberg, B., Richter, C. F., 1944. Frequency of earthquakes in California. *Bulletin of the Seismological Society of America*, *34*(4), 185-188.

HAZUS, 2012. *HAZUS–MH 2.1: Technical Manual*. User's Manual and Documentation, Federal Emergency Management Agency.

Hwang, H., Jernigan, J., Lin, Y. W., 2000. Evaluation of seismic damage to Memphis bridges and highway systems. *Journal of Bridge Engineering, 5*(4), 322-330.

Jayaram, N., Baker, J., 2010. Efficient sampling and data reduction techniques for probabilistic seismic lifeline risk assessment. *Earthquake Engineering and Structural Dynamics, 39*(10), 1109–1131.

Jenelius, E., Petersen, T., Mattsson, L. G., 2006. Importance and exposure in road network vulnerability analysis. *Transportation Research Part A: Policy and Practice 40*(7), 537-560.

Jenelius, E., (2010). User inequity implications of road network vulnerability. *Journal of Transport and Land Use 2*(3), 57-73.

Jenelius, E., Mattsson, L., 2015. Road network vulnerability analysis: Conceptualization, implementation and application. *Computers, Environment and Urban Systems, 49*, 136-147.

Karim, K., Yamazaki, F., 2003. A simplified method of constructing fragility curves for highway bridges. *Earthquake Engineering and Structural Dynamics 32(10)*: 1603-1626.

Kassir, M., Ghosn, M., 2002. Chloride-induced corrosion of reinforced concrete bridge decks. *Cement and Concrete Research, 32*(1), 139-143.

Kendall, A., Keoleian, G., Helfand, G., 2008. Integrated life-cycle assessment and life-cycle cost analysis model for concrete bridge deck applications. *Journal of Infrastructure Systems, 14*(3), 214-222.

Kim, Y. J., Yoon, D. K., 2010. Identifying Critical Sources of Bridge Deterioration in Cold Regions through the Constructed Bridges in North Dakota. *Journal of Bridge Engineering 15*(5), 542-552

Koch, H., Brongers, M., Thompson, N., Virmani, Y., Payer, J., 2001. *Corrosion Cost and Preventive Strategies in the United States.* CC Technologies Laboratories, Dublin, OH, USA – Report R315-01. Houston, TX, USA, NACE Int.

Kumar, R., Gardoni, P., Sanchez-Silva, M., 2009. Effect of cumulative seismic damage and corrosion on the life-cycle cost of reinforced concrete bridges. *Earthquake Engineering and Structural Dynamics*, *38*, 887-905.

LeBlanc, L., Morlok, E., Pierskalla, W., 1975. An efficient approach to solving the road network equilibrium traffic assignment problem. *Transportation Research, 9*(5), 309-318.

Lemma, M. S., Gervásio, H., Pedro, J. O., Rigueiro, C., da Silva, L. S., 2020. Enhancement of the life-cycle performance of bridges using high-strength steel. *Structure and Infrastructure Engineering 16*(4): 772-786.

Maibach, M., Peter, M.; Sutter, D., 2006. *Analysis of operating cost in the EU and the US. Annex 1 to Final Report of COMPETE Analysis of the contribution of transport policies to the competitiveness of the EU economy and comparison with the United States*. Funded by European Commission – DG TREN. Karlsruhe, Germany.

Marsh, P., Frangopol, D. M., 2008. Reinforced concrete bridge deck reliability model incorporating temporal and spatial variations of probabilistic corrosion rate sensor data. *Reliability Engineering and System Safety 93*(3): 394-409.

Mackie, K. R., Stojadinović, B., 2007. R-factor parameterized bridge damage fragility curves. *Journal of Bridge Engineering 12(4)*: 500-510.

Mackie, K., Wong J., Stojadinovic, B., 2009. Post-earthquake bridge repair cost and repair time estimation methodology. *Earthquake Engineering and Structural Dynamics 39*(3), 281-301

Mackie, K., 2010. Sensitivities in Repair Cost and Repair Time Metrics for Seismic Bridge Response. *Structure Congress 2010*, Orlando, Florida (US), May 12-15, 2010.

Mander, J., 1999. Fragility curve development for assessing the seismic vulnerability of highway bridges. In: *Research Progress and Accomplishments 1997-1999,* MCEER, University at Buffalo, NY, USA.

Marí, A., Bairán, J., 2008. Evaluation of the response of concrete structures along their service life by nonlinear evolutive analysis methods. *First International Symposium on Life-Cycle Engineering* (IALCEE'08), Varenna, Lake Como, Italy, June 11-14. In: *Life-Cycle Civil Engineering: Proceedings of the International Symposium on Life-Cycle Civil Engineering, IALCEE'08*. F. Biondini, D.M. Frangopol (Eds.), CRC Press/Balkema, Taylor & Francis Group, London, UK.

McGuire, R., 2007. *Seismic Hazard and Risk Analysis.* EERI.

Meletti, C., Galadini, F., Valensise, G., Stucchi, M., Basili, R., Barba, S., Vannucci, G., Boschi, E., 2008. A seismic source zone model for the seismic hazard assessment of the Italian territory. *Tectonophysics, 450*(1-4), 85-108.

Ministry of Economy and Finance (MEF) (2018). Public debt report 2018, Treasury Department, Directorate II. <http://www.dt.mef.gov.it/en/debito_pubblico/presentazioni_studi_relazioni/archivio_presentazioni/elem_0008.html>. Last access: June 25th, 2020.

Mirzaei, Z., Adey, B. T., 2015. Investigation of the use of three existing methodologies to determine optimal life-cycle activity profiles for bridges. *Structure and Infrastructure Engineering 11*(11): 1484-1509

Moehle, J., Deierlein, G., 2004. A framework methodology for performance-based earthquake engineering. *13th World Conference of Earthquake Engineering*, Vancouver, Canada, August 1-6, 2004.

MPS Working Group, 2004. *Redazione della mappa di pericolosità sismica prevista dall'Ordinanza PCM 3274 del 20 marzo 2003. Rapporto conclusivo per il Dipartimento della Protezione Civile*, INGV, Milano-Roma, April 2004 (MPS04), 65 pp.+ 5 appendices (In Italian).

Navarro, I. J., Yepes, V., Martí, J. V., 2018. Social life cycle assessment of concrete bridge decks exposed to aggressive environments. *Environmental Impact Assessment Review 72*: 50-63.

Odgaard, T., Kelly, C., Laird, J., 2005. *HEATCO Work Package 3: Current practice in project appraisal in Europe - Deliverable 1*. European Commission EC-DG TREN.

Open Data Portal Regione Lombardia, 2016. < https://www.dati.lombardia.it>. Last access: March 1st, 2020.

Ozbay, K., Jawad, D., Parker, N., Hussain, S., 2004. Life-cycle cost analysis: State of the practice versus state of the art. *Transportation Research Record: Journal of the Transportation Research Board, 1864*(1), 62-70.

Padgett, J. E., DesRoches, R., 2007. Bridge functionality relationships for improved seismic risk assessment of transportation networks. *Earthquake Spectra 23*(1), 115-130.

Porter, K., 2003. An Overview of PEER's Performance-Based Earthquake Engineering Methodology. *9th International Conference on Applications of Statistics and Probability in Civil Engineering*, San Francisco, CA, USA, CERRA.

QGIS, 2016. *Open source geospatial foundation project*. QGIS geographic information system.

Rao, A., Lepech, M., Kiremidjian, A., 2017. Development of time-dependent fragility functions for deteriorating reinforced concrete bridge piers. *Structure and Infrastructure Engineering, 13*(1), 67-83.

Rackwitz, R., Lentz, A., Faber, M., 2005. Socio-economically sustainable civil engineering infrastructures by optimization. *Structural safety*, *27*(3), 187-229.

Rackwitz, R., 2006. The effect of discounting, different mortality reduction schemes and predictive cohort life tables on risk acceptability criteria. *Reliability Engineering & System Safety, 91*(4), 469-484.

Regione Lombardia , 2016. Programma Regionale Mobilità e Trasporti (PRMT). *Struttura Programma Regionale della Mobilità e dei Trasporti–DG Infrastrutture e Mobilità*, *Milano, Italy.*

Rokneddin, K., Ghosh, J., Dueñas-Osorio, L., Padgett, J. E., 2014. Seismic reliability assessment of aging highway bridge networks with field instrumentation data and correlated failures, II: Application. *Earthquake Spectra 30*(2), 819-843.

Rupi, F., Bernardi, S., Rossi, G., Danesi, A., 2015. The Evaluation of Road Network Vulnerability in Mountainous Areas: A Case Study. *Networks and Spatial Economics 15*(2): 397-411.

Santander, C. F., Sanchez-Silva, M., 2008. Design and maintenance programme optimization for large infrastructure systems. *Structures and Infrastructure Engineering, 4*(4), 297-309.

Shekhar, S., Ghosh, J., Padgett, J. E., 2018. Seismic life-cycle cost analysis of ageing highway bridges under chloride exposure conditions: modelling and recommendations. *Structure and Infrastructure Engineering 14*(7): 941-966.

Shekhar, S., Ghosh, J., 2020. A metamodeling based seismic life-cycle cost assessment framework for highway bridge structures. *Reliability Engineering and System Safety 195*: 106724

Shinozuka, M., Murachi, Y., Dong, X., Zhou, Y., Orlikowski, M., 2003. Effect of seismic retrofit of bridges on transportation networks. *Earthquake Engineering and Engineering Vibration, 2*(2), 169-179.

Shiraki, N., Shinozuka, M., Moore, J., Chang, S., Kameda, H., Tanaka, S., 2007. System risk curves: Probabilistic performance scenarios for highway networks subject to earthquake damage. *Journal of Infrastructure Systems, 13*(1), 43-54.

Sierra, L. A., Yepes, V., García-Segura, T., Pellicer, E., 2018. Bayesian network method for decision-making about the social sustainability of infrastructure projects. *Journal of Cleaner Production 176*: 521-534

Son, Y., Sinha, K., 1997. Methodology to estimate user costs in Indiana Bridge Management System. *Transportation Research Record*, *1597*(1), 43-51.

Stein, S., Young, G., Trent, R., Pearson, D., 1999. Prioritizing scour vulnerable bridges using risk. *Journal of Infrastructure Systems, 5*(3), 95-101.

Stergiou, E. C., Kiremidjian, A. S., 2010. Risk assessment of transportation systems with network functionality losses. *Structure and Infrastructure Engineering*, 6(1-2): 111-125.

Sullivan, J. L., Novak, D. C., Aultman-Hall, L., Scott, D. M., 2010. Identifying critical road segments and measuring system-wide robustness in transportation networks with isolating links: A link-based capacity-reduction approach. *Transportation Research Part A: Policy and Practice 44*(5), 323-336.

Thoft-Christensen, P., 2009. Life-cycle cost-benefit (LCCB) analysis of bridges from a user and social point of view. *Structure and Infrastructure Engineering, 5*(1), 49-57.

Thoft-Christensen, P., 2012. Infrastructures and life-cycle cost-benefit analysis. *Structure and Infrastructure Engineering, 8*(5), 507-516.

Titi, A., Biondini, F., 2014.Probabilistic seismic assessment of multistory precast concrete frames exposed to corrosion, *Bulletin of Earthquake Engineering*, Springer,**12**(6), 2014, 2665–2681

Titi, A., Biondini, F., Frangopol, D. M., 2015. Seismic resilience of deteriorating concrete structures. *Structures Congress 2015*, Portland, OR, USA, April 23-25, 2015. In: *Proceedings of the 2015 Structures Congress*, N. Ingraffea, M. Libby (Eds.), ASCE.

Titi, A., Biondini, F., 2016. On the accuracy of diffusion models for life-cycle assessment of concrete structures. *Structure and Infrastructure Engineering 12*(9): 1202-1215.

Tsionis, G., Fardis, M.N., 2014. Fragility functions of road and railway bridges. In K. Pitilakis, E. Crowley, and A. M. Kaynia (eds.) *SYNER-G: Typology definition and fragility functions for physical elements at seismic risk*, Geotechnical, Geological and Earthquake Engineering Vol 27, Springer Netherlands, Netherlands, pp. 259-297.

Twumasi-Boakye, R., Sobanjo, J. 2017. Evaluating transportation user costs based on simulated regional network models. *Transportation Research Record, 2612*(1), 121-131.

Val, D., Melchers, R., 1997. Reliability of deteriorating RC slab bridges. *Journal of Structural Engineering, 123*(12), 1638-1644.

Val, D., Stewart, M., 2003. Life-cycle cost analysis of reinforced concrete structures in marine environments. *Structural Safety, 25*(4), 343-362.

Wardrop, J., 1952. Some theoretical aspects of road traffic research. *Proceedings of the Institution of Civil Engineers*, *1*(3), 325-362.

Yang, D.Y., Frangopol, D.M., 2020. Life-Cycle Management of Deteriorating Bridge Networks with Network-Level Risk Bounds and System Reliability Analysis. *Structural Safety 83*: 101911.

Yavuz, F., Attanayake, U., Aktan, H. Economic Impact on Surrounding Businesses due to Bridge Construction. *Procedia Computer Science 109*:108-115.

Zanini, M. A., Faleschini, F., Pellegrino, C., 2017. Probabilistic seismic risk forecasting of aging bridge networks. *Engineering structures 136*: 219-232.

Zhang, D., Ye, F., Yuan, J., 2013. Life-cycle Cost Analysis (LCCA) on Steel Bridge Pavement Structural Composition. *Procedia - Social and Behavioral Sciences 96*: 785-789.

Zhong, J., Gardoni, P., Rosowsky, D., 2012. Seismic fragility estimates for corroding reinforced concrete bridges. *Structure and Infrastructure Engineering, 8*(1): 55-69.

Zhou, Y., Banerjee, S., Shinozuka, M., 2010. Socio-economic effect of seismic retrofit of bridges for highway transportation networks: a pilot study. *Structure and Infrastructure Engineering, 6*(1-2), 145-157.

Zhu, S., Levinson, D., 2015. Do people use the shortest path? An empirical test of wardrop's first principle. *PLoS ONE, 10*(8), e0134322.

Table 1. Daily *DDC* and *VOC* for the closure of all the bridges on a route of regional interest.

Route	Cities	Light traffic [€/day]		Heavy traffic [€/day]	
		DDC	*VOC*	*DDC*	*VOC*
1	Pavia-Lodi-Crema	$5.94 \cdot 10^4$	$9.61 \cdot 10^3$	$1.24 \cdot 10^3$	-1.03
2	Crema-Cremona	4.24	233.61	0	-7.45
3	Pavia-Cremona	$2.12 \cdot 10^5$	$1.13 \cdot 10^4$	$1.92 \cdot 10^4$	$3.62 \cdot 10^4$

Table 2. Statistical parameters of the truncated Gutenberg-Richter distribution for the seismogenic zones of interest (MPS Working Group 2004)

Zone	Dominant Faulting Mechanism	b	$m_{\min}$	$m_{\max}$	$\nu_{m \geq m_{\min}}$
906	Reverse	1.14	4.76	6.60	0.11
907	Reverse	1.71	4.76	6.14	0.04
911	Strike-slip	1.47	4.76	6.14	0.05
913	Undetermined	1.80	4.76	6.14	0.07

Table 3. Classification and median fragility values for the undamaged bridges in the network.

Bridge	Material	Type	Length ≥ 150 m	HAZUS	$\exp(\bar{\lambda}_{s,b})$	
					Slight	Extensive
1	RC	Continuous	No	HWB10	0.60	1.10
2	RC	Continuous	Yes	HWB1	0.40	0.70
3	RC	Continuous	Yes	HWB1	0.40	0.70
4	RC	Continuous	No	HWB10	0.60	1.10
5	Steel	Continuous	No	HWB15	0.75	0.75
6	RC	Arch bridge	No	HWB28	0.80	1.20
7	RC	Single span	No	HWB3	0.80	1.20
8	RC	Arch bridge	No	HWB28	0.80	1.20
9	Steel	Continuous	No	HWB15	0.75	0.75
10	RC	Arch bridge	No	HWB28	0.80	1.20
11	RC	Arch bridge	No	HWB28	0.80	1.20
12	RC	Continuous	No	HWB10	0.60	1.10
13	RC	Continuous	Yes	HWB1	0.40	0.70
14	RC	Continuous	No	HWB28	0.80	1.20
15	RC	Gerber	Yes	HWB1	0.40	0.70
16	Steel	Continuous	Yes	HWB1	0.40	0.70
17	RC	Single span	No	HWB3	0.80	1.20
18	RC	Single span	No	HWB3	0.80	1.20
19	RC	Single span	No	HWB3	0.80	1.20
20	RC	Continuous	No	HWB10	0.60	1.10
21	RC	Continuous	Yes	HWB1	0.40	0.70

Table 4. Statistical parameters of the probability distributions of the recovery model random variables for different damage states s_b: Beta(a,b) distribution of shape parameter $\omega\in[0;1]$; Uniform distribution of shape parameter $\rho\geq0$; Uniform distribution of total recovery interval $\Delta T_{r,b}$.

Damage State	ω		ρ		$t_{i,b}$ [days]		$t_{r,b}$ [days]	
	a	b	Min	Max	Min	Max	Min	Max
Slight	2	8	1.0	3.0	5	30	5	120
Extensive	8	2	2.5	7.5	5	30	120	270

Table 5. Annual rate of exceedance of a 1M € user cost expenditure for different time of occurrence of the seismic event.

Time of occurrence t_0 [years]	Annual rate of exceedance $\nu_{C\geq c}$
0	$1.24\cdot10^{-6}$
10	$1.25\cdot10^{-6}$
20	$1.30\cdot10^{-6}$
30	$1.34\cdot10^{-6}$
40	$1.50\cdot10^{-6}$
50	$1.54\cdot10^{-6}$
60	$6.33\cdot10^{-6}$
70	$6.75\cdot10^{-6}$
80	$7.40\cdot10^{-6}$
90	$1.10\cdot10^{-5}$
100	$5.19\cdot10^{-5}$

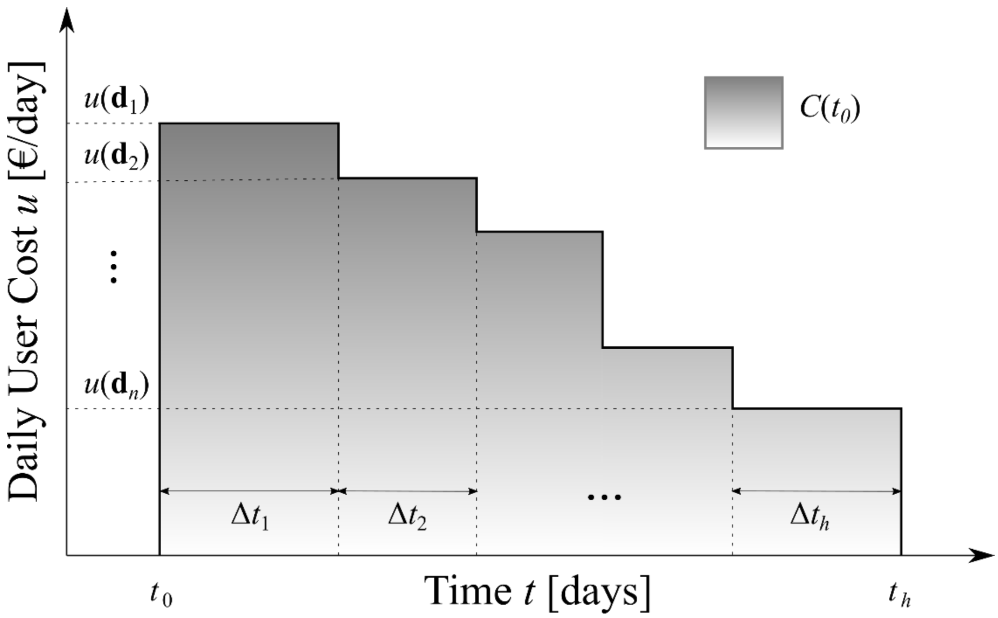

Figure 1. Cumulative cost profile.

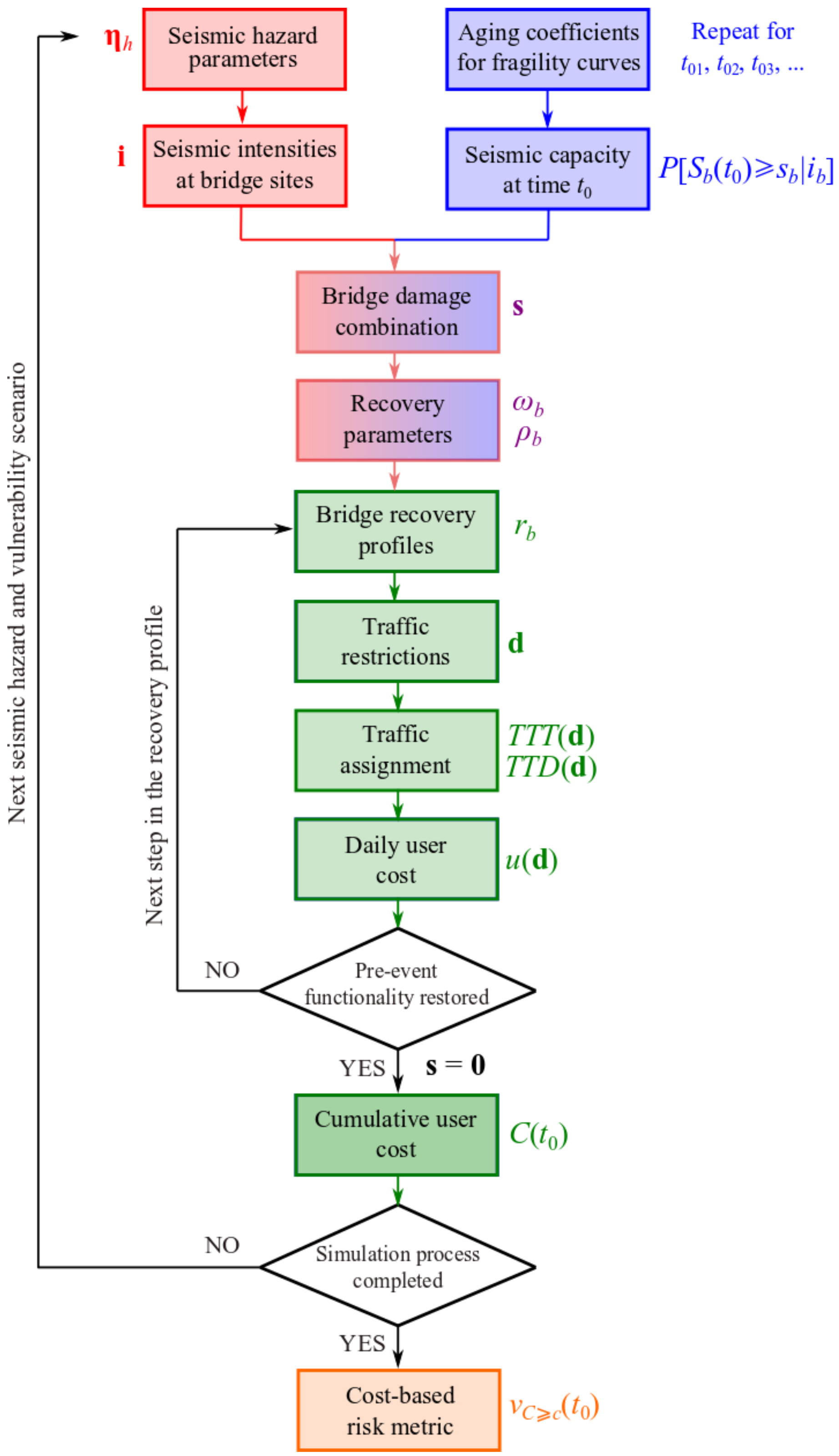

Figure 2. Flowchart of the proposed life-cycle approach.

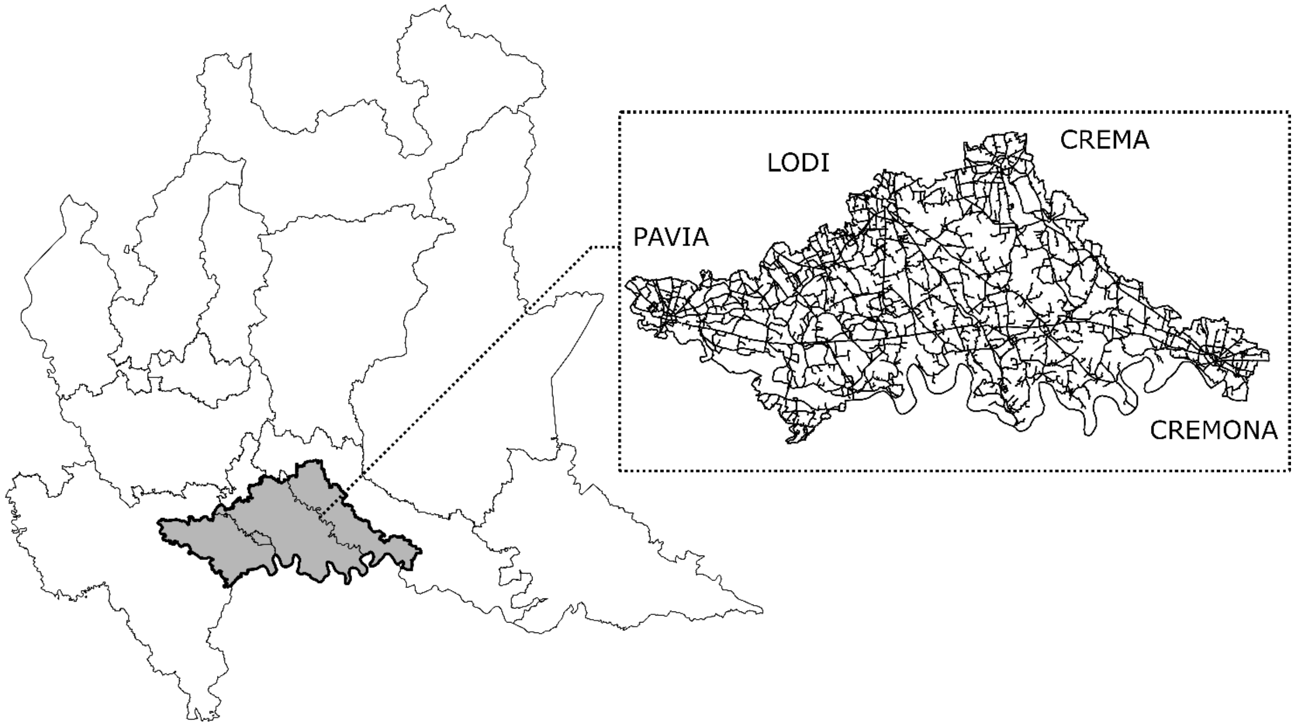

Figure 3. Benchmark network layout in Lombardy region

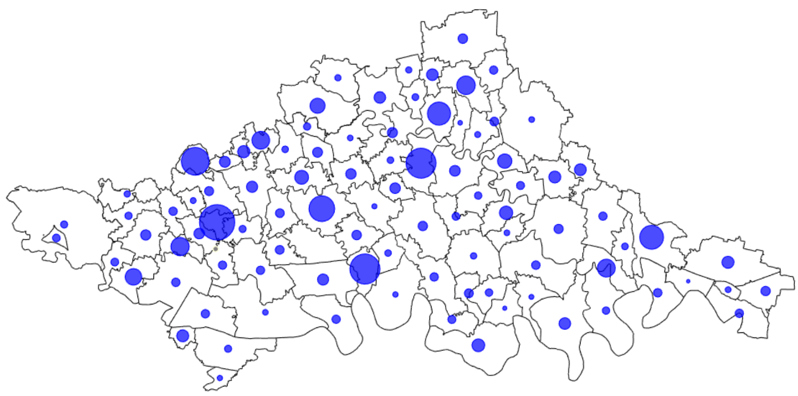

(a)

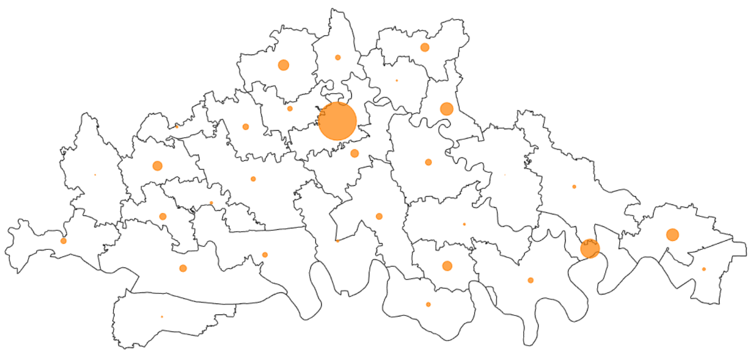

(b)

Figure 4 - Traffic zones and originated trip densities for (a) light and (b) heavy vehicles.

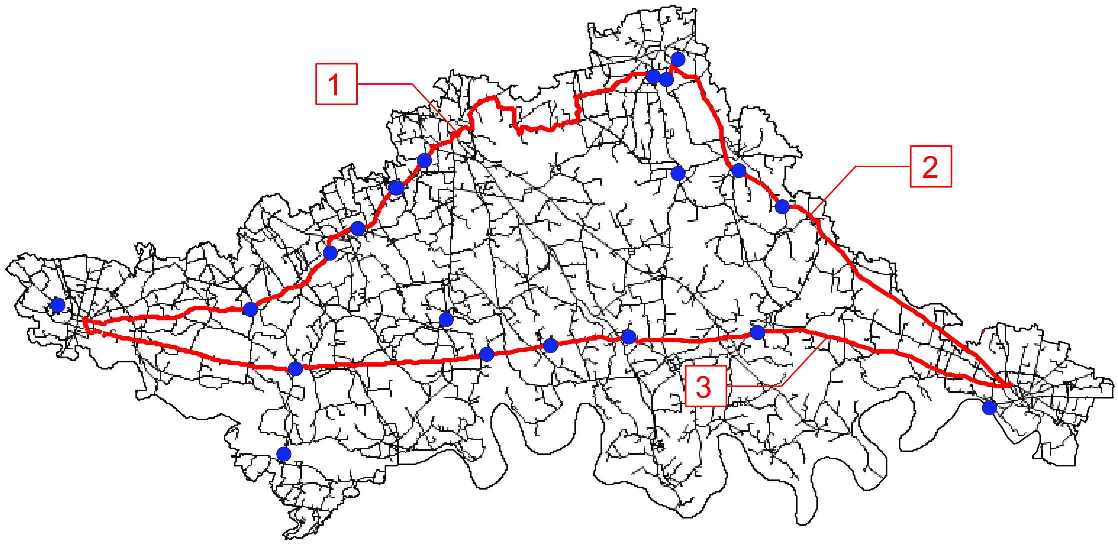

Figure 5 –Bridge locations within the road system (filled dots) and roads of regional interest (thick lines).

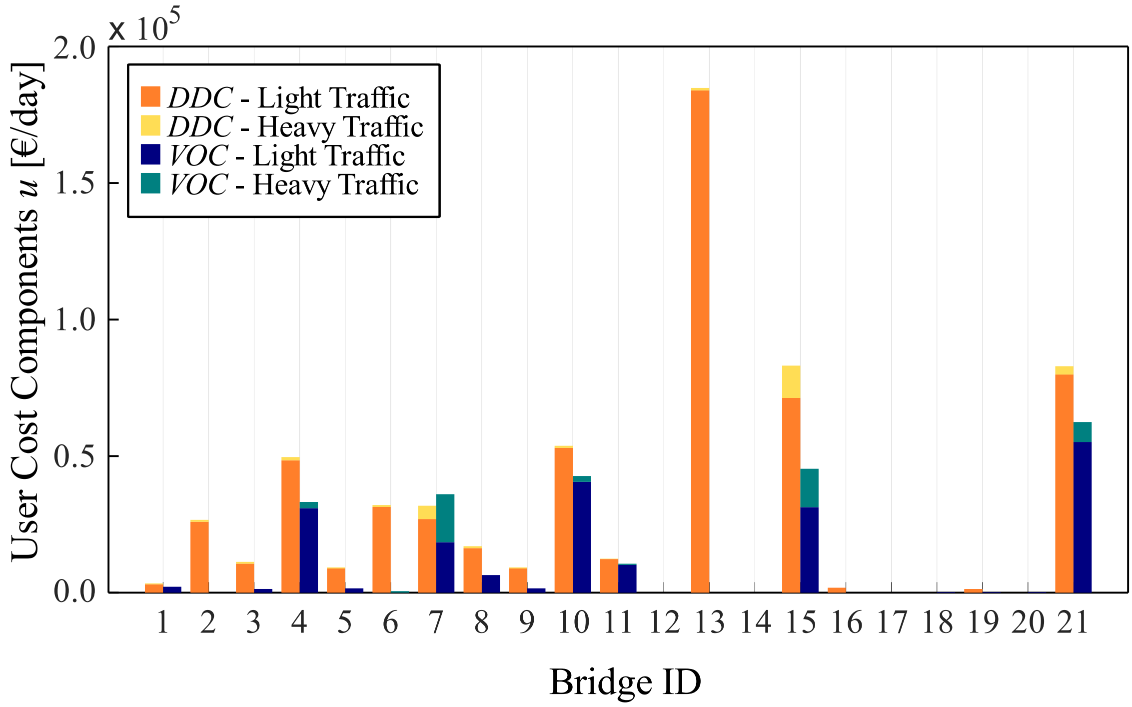

Figure 6 – Daily *DDC* and *VOC* under full closure of a single bridge.

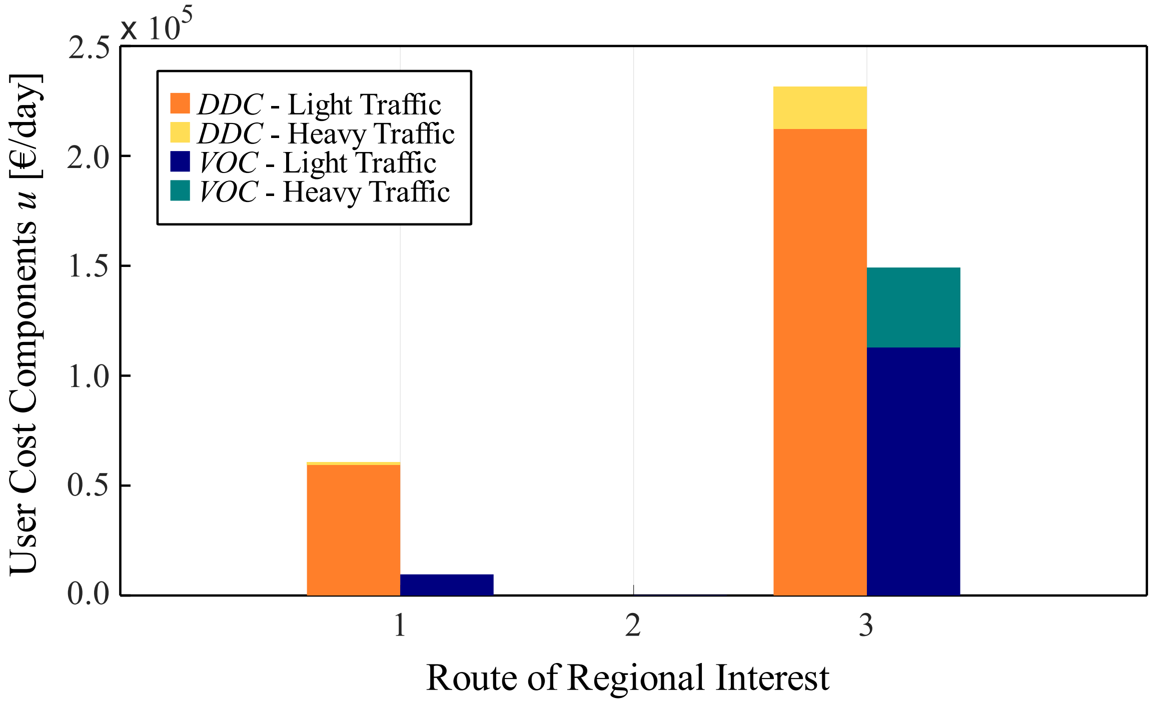

Figure 7 – Daily *DDC* and *VOC* under full closure of one route of regional interest.

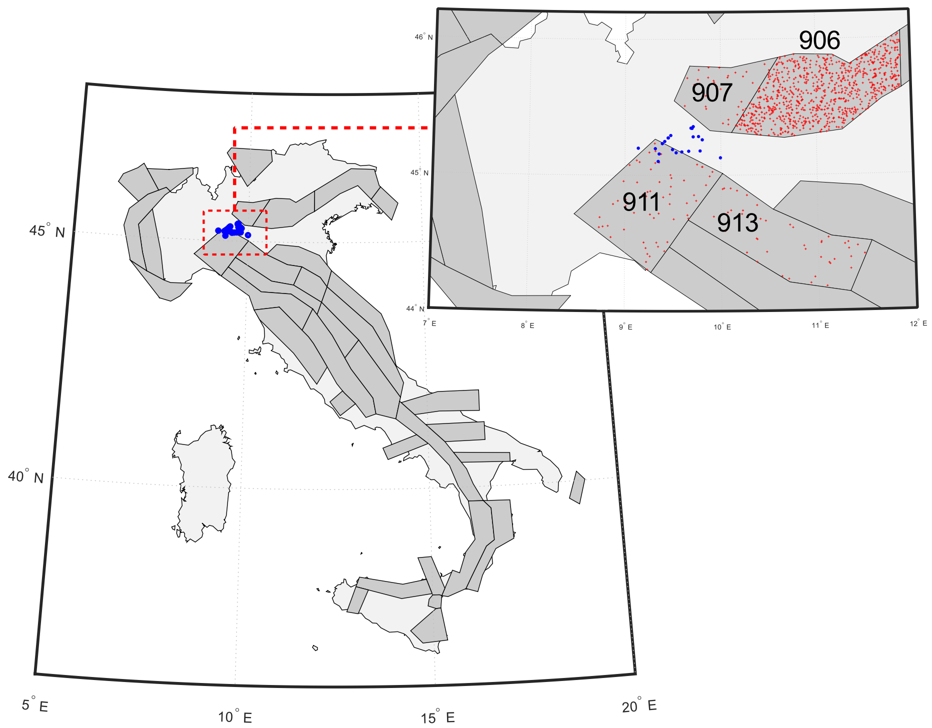

Figure 8 – ZS9 seismogenic zonation (dark grey areas), bridge locations (dots) and realizations of epicenters locations (small dots in area sources).

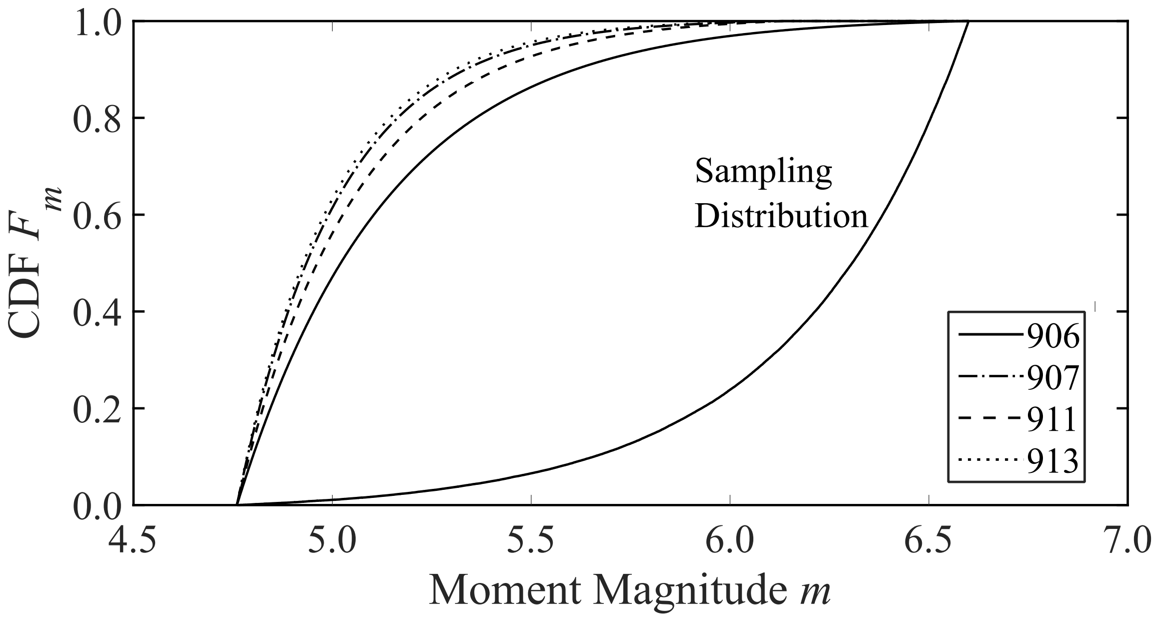

Figure 9 – CDFs of active area sources and Importance Sampling distribution.

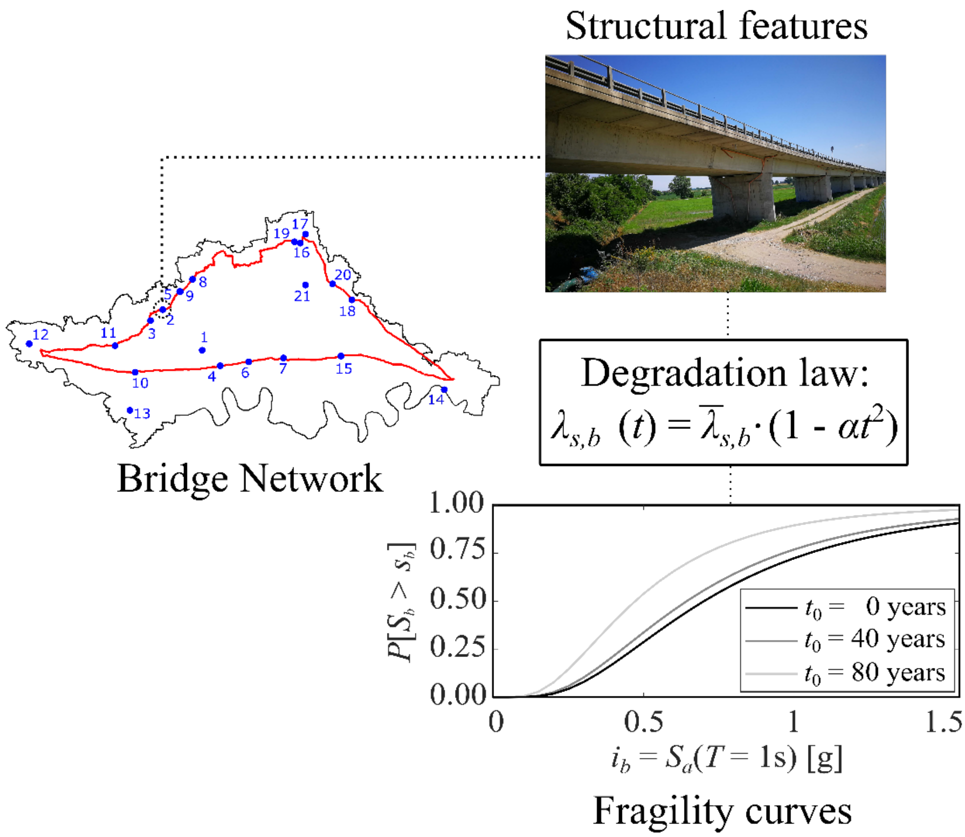

Figure 10 – Time-variant fragility curves of individual bridges in the network.

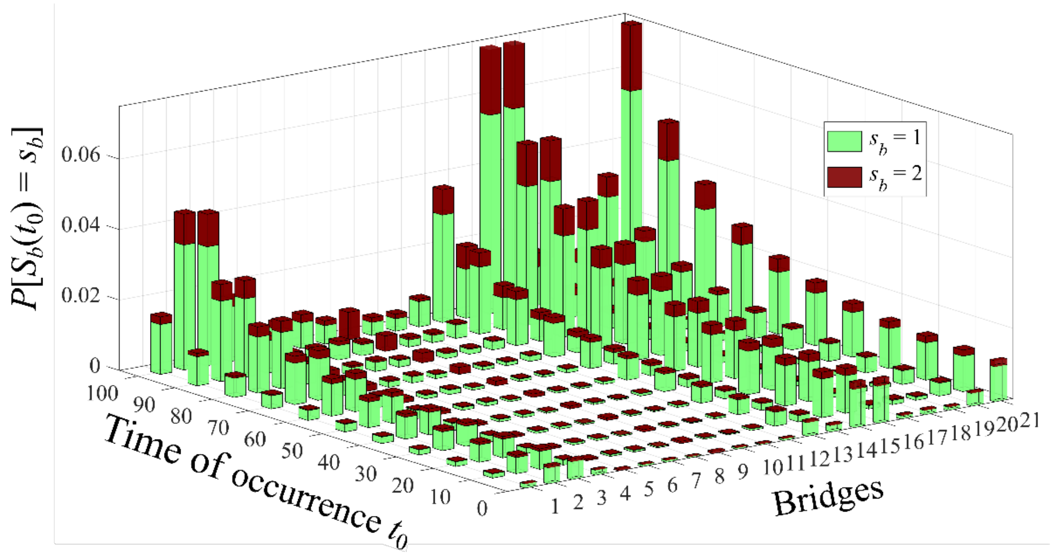

Figure 11 – Empirical probability of exceedance of damage states s_b=1 and s_b=2

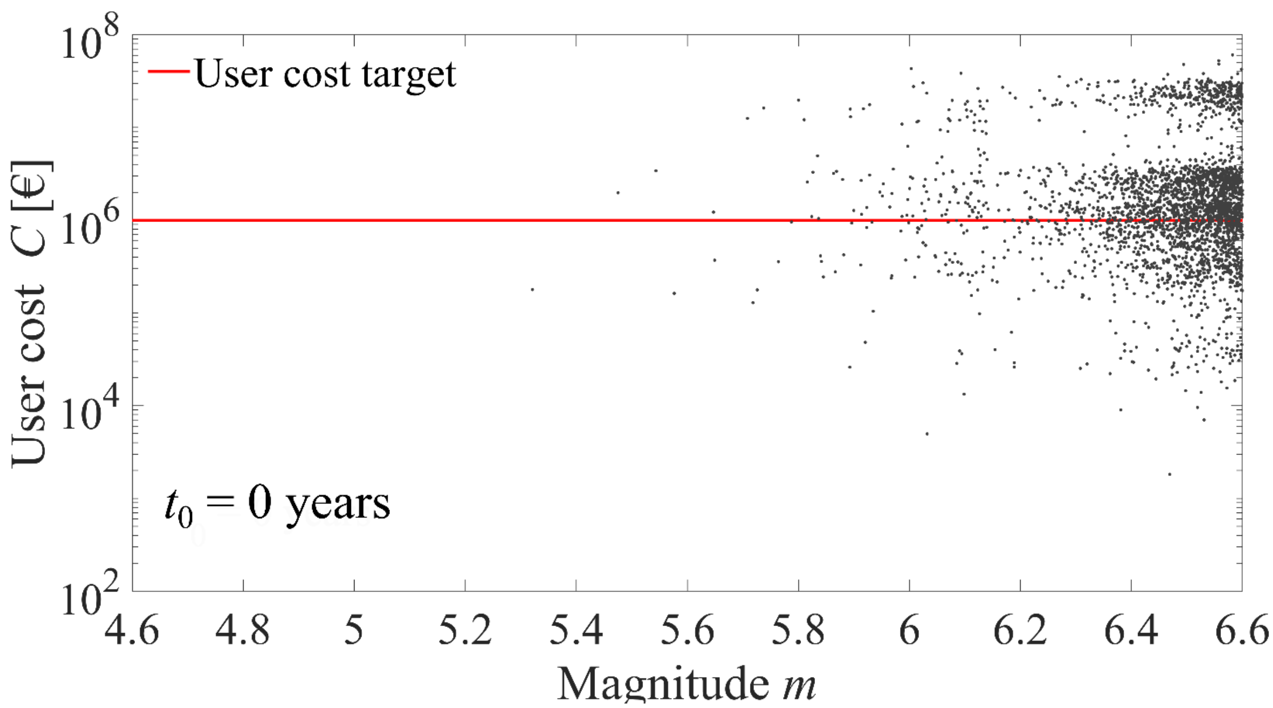

(a)

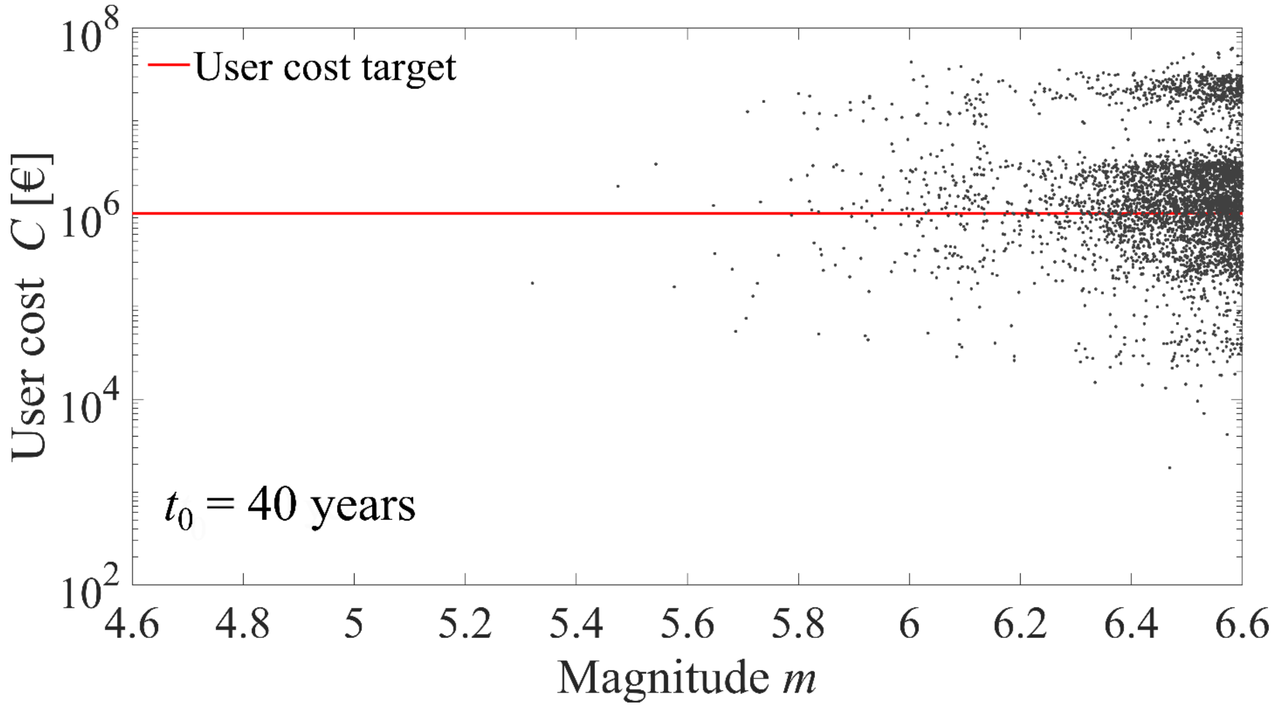

(b)

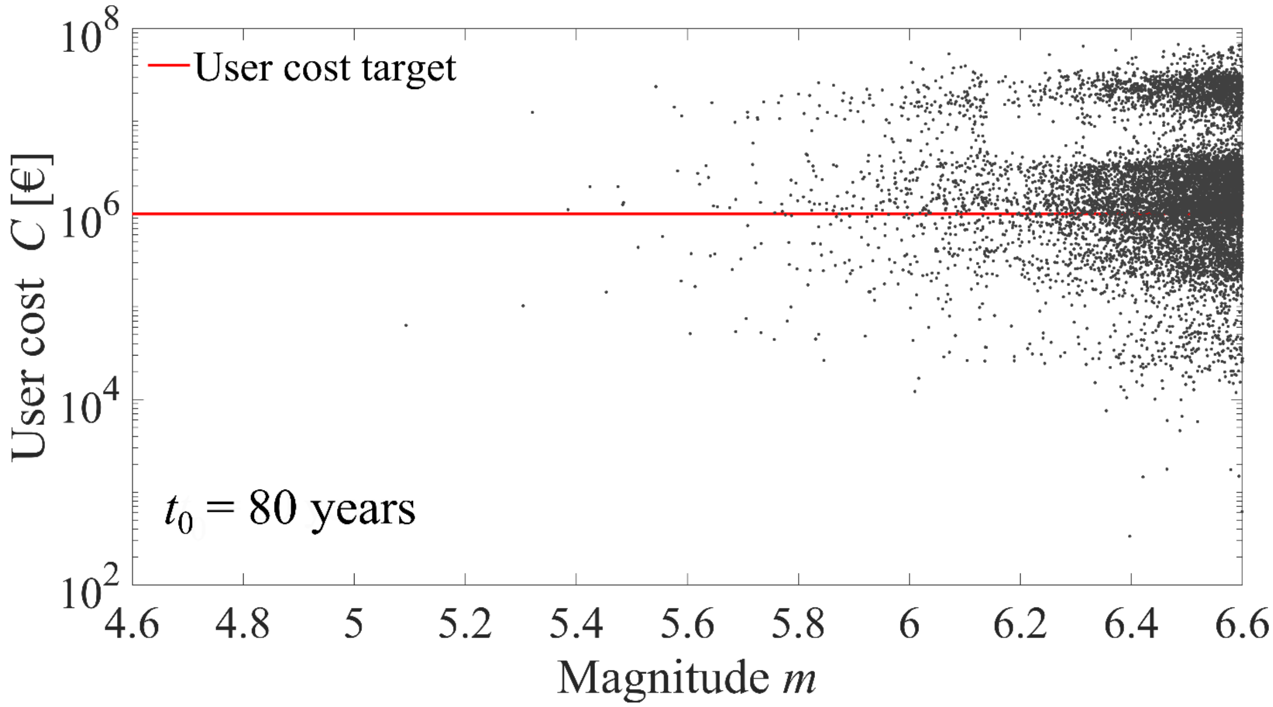

(c)

Figure 12 – User cost realizations compared with target user cost versus causative moment magnitude for occurrence time at 0 (a), 40 (b) and 80 (c) years.

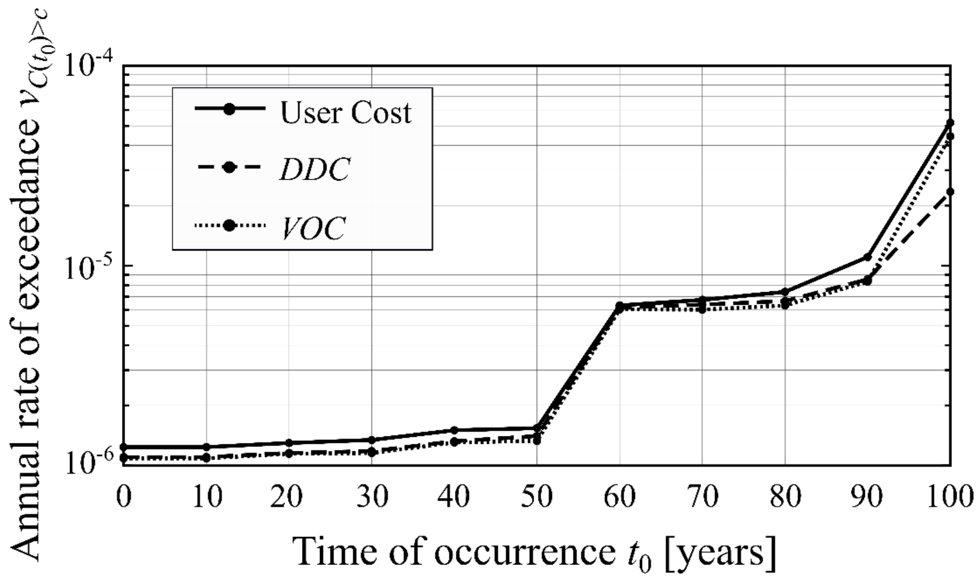

Figure 13 – Annual rate of exceedance of total user cost, DDC and VOC for different times of occurrence of the earthquake.

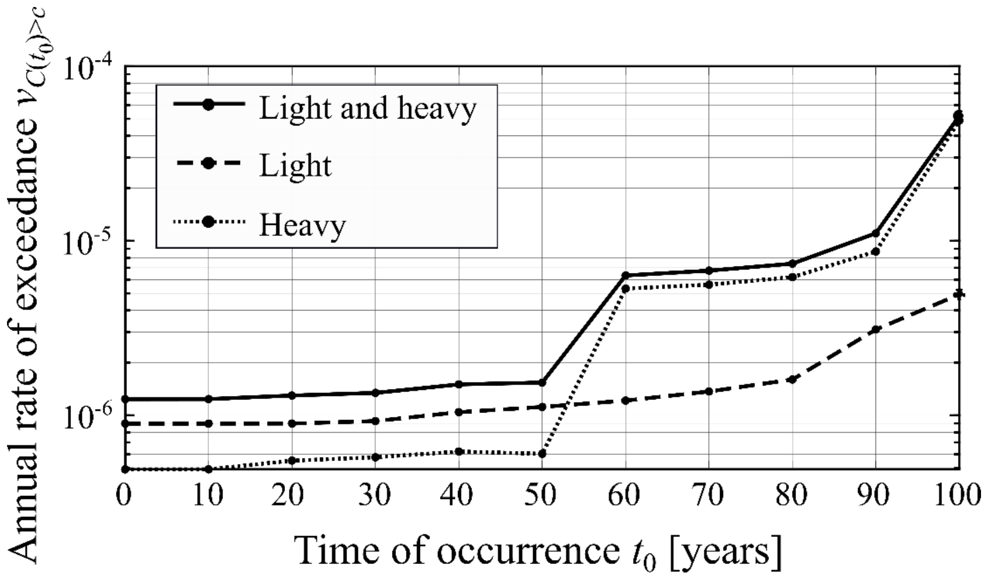

Figure 14 – Annual rate of exceedance of total user cost for light, heavy and both light and heavy vehicles for different times of occurrence of the earthquake.

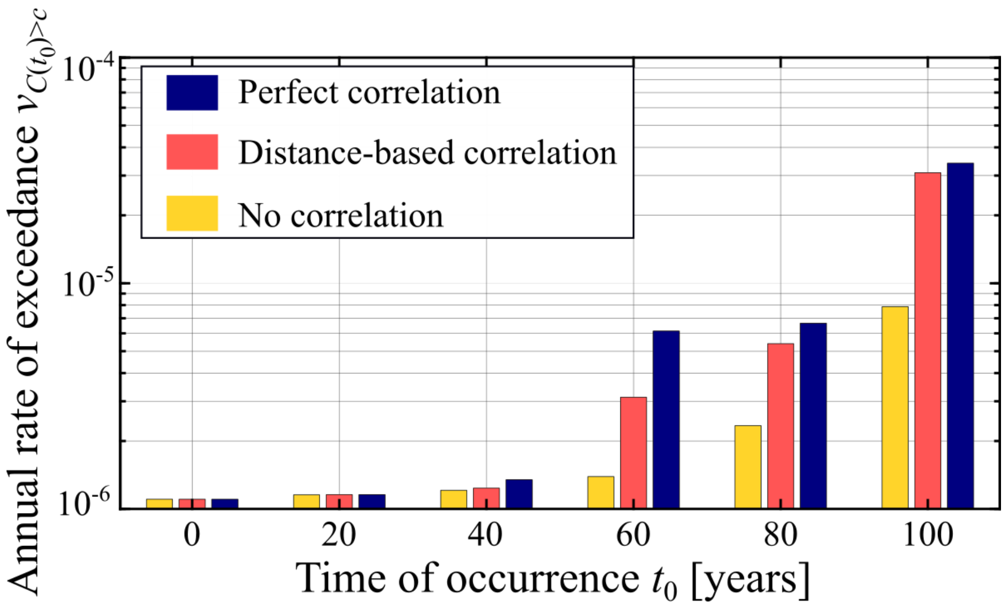

Figure 15 – Annual rate of exceedance of DDC for perfect, distance-based and no correlation for different times of occurrence of the earthquake.

.